

# Geometric and fluctuational divergences in the linear response of coherently driven microcavity polaritons and their relation to superfluidity

I. Timofeev , R. Juggins , and M. H. Szymańska *Department of Physics and Astronomy, University College London Gower Street, London WC1E 6BT, United Kingdom*

(Received 24 April 2023; revised 7 November 2023; accepted 17 November 2023; published 11 December 2023)

We consider the possibility of superfluid behavior in a coherently driven, dissipative microcavity polariton system in gapless spectrum regimes. Previous work demonstrated the absence of such behavior for gapped spectra via a linear response analysis. The system can, however, be tuned to possess a gapless spectrum in special cases, leaving open the possibility of superfluid behavior. Here we show the absence of superfluidity in all regimes; we find a divergent linear response in the system's gapless regimes, which may be linked to phase-transition behavior. This indicates that the gapless spectrum is related to phase instability and not superfluid-enabling massless modes.

DOI: [10.1103/PhysRevB.108.214513](https://doi.org/10.1103/PhysRevB.108.214513)

## I. INTRODUCTION

Superfluidity is a classic phenomenon in quantum mechanics. First discovered in 1937 in liquid helium-4 [1,2], it is characterized by a series of unusual hydrodynamic properties such as vanishingly small viscosity, the inability to rotate except in quantized vortices, and the flow of metastable currents that persist for astronomical timescales. It has been widely studied and found to occur in a variety of other systems, including helium-3, ultra-cold bosonic atoms, and charged Cooper pairs in superconductors [3,4].

While historical research on superfluidity has concentrated on examples in thermal equilibrium, in recent years driven-dissipative systems, which never thermalize due to constant decay and must be pumped to maintain a steady state, have begun to generate substantial interest. Examples of such systems are numerous, including Bose-Einstein condensates (BEC) of photons [5,6], cold atoms coupled to photonic modes in optical cavities [7], and cavity arrays [8–10]. Of particular note are microcavity polaritons [11–13], which are two-dimensional bosonic quasiparticles made of photons trapped in a cavity strongly coupled to excitons in a quantum well. While we shall focus here on their more fundamental properties, in recent years microcavity polaritons have found many practical applications [14–16] including spintronics [17–19], lasing [20–22], and optical circuits [23,24].

Polariton experiments have observed a number of effects usually associated with superfluidity, such as the suppression of scattering for flow past a defect [25–27], metastable persistent currents [28], and quantized vortices [29]. The question of how superfluidity may occur in these out-of-equilibrium systems has proved contentious [29–35], however, and it is

unclear whether all the effects seen in equilibrium will continue to apply [11,36,37]. Of particular importance when classifying these systems is that the classic notion of superfluidity groups together multiple behaviors into a “complex of phenomena” [38]. While flow without viscosity is perhaps the most famous of these, irrotationality of superflow is crucial for characterizing a superfluid state. Unlike the former property, which is only approximately true at finite temperature and provides no clear distinction between true superfluids and generic low viscosity systems, the definition of a superfluid as a macroscopic quantum state in which the bulk does not rotate provides a precise description. This property is encoded in the response of a system to longitudinal and transverse perturbations. Given that superfluids exhibit the former but not the latter, if there exists a difference between the two the system in question must contain a superfluid component. Indeed, this has become a standard definition of superfluidity [31,39–44].

The properties of microcavity polaritons are heavily dependent on how the system is pumped, that is, on how photons are injected into the cavity. When this occurs incoherently, meaning photons are injected far off-resonance, then relaxation processes involving excitons and photons will under the right conditions lead to the “condensation” of polaritons into a low-energy state [45]. This process involves the spontaneous breaking of the  $U(1)$  phase symmetry of the macroscopic wave function, leading to a Goldstone mode in the excitation spectrum of the system [46,47]. In a theoretical study of the longitudinal and transverse response functions of an incoherently driven system using a Keldysh path integral technique [31], it was found that the gapless excitation spectrum allowed superfluidity to survive despite the driven-dissipative nature of the system.

Alternatively, polaritons may be pumped coherently, meaning they are injected at a specific energy and momentum, and can form a macroscopic state with a phase fixed to that of the external pump [48]. Because of this phase fixing, the excitation spectrum in such a system is typically gapped.

*Published by the American Physical Society under the terms of the Creative Commons Attribution 4.0 International license. Further distribution of this work must maintain attribution to the author(s) and the published article's title, journal citation, and DOI.*

Despite this, experiments have observed that coherently pumped polaritons can flow past a defect with vanishing dissipation; this, together with theoretical analysis speculatively applying the Landau criterion to the real part of the polariton spectrum [49,50], has been claimed as evidence of superfluidity [25]. The Landau criterion, however, is applicable only to conservative systems with purely real energy spectra. By applying the Keldysh path integral technique to directly calculate the longitudinal and transverse responses of coherently pumped polaritons, two of the present authors found these responses to be equal in all regimes with a gapped excitation spectrum, indicating an absence of superfluidity and underscoring the inadequacy of the Landau criterion for driven-dissipative systems [51].

For special choices of system parameters, however, coherently pumped polaritons may be induced to possess a gapless spectrum, suggesting the possibility of superfluid behavior in these regimes. In this paper, we derive the mean-field responses at such points in parameter space, showing that while an anisotropic (nonzero momentum) pump yields a divergent linear response, an isotropic (zero momentum) pump leads to a pure superfluid one. However, we further demonstrate that, when perturbative corrections are included, coherently driven polaritons do not exhibit superfluidity in any regime. By analyzing the system from the point of view of catastrophe theory, we show that the anisotropic mean-field divergence of the response is physical and related to bifurcations in the system order parameter. Such bifurcations are also responsible for the gapless mode, which is shown to be due to the appearance of a “non-Morse critical point” of the action. Finally, performing perturbative calculations to  $O(\hbar^2)$ , we demonstrate that higher-order terms of the perturbation expansion in both isotropic and anisotropic cases diverge in the gapless regime due to these points in fact corresponding to phase transitions and the condensate density diverging; this indicates that perturbation theory is not rigorously applicable and that the mean-field superfluidity result is misleading.

In Sec. II of this paper, we recapitulate the theoretical debate around superfluidity in coherently driven polaritons, explaining the attempted applications of the Landau criterion [49,50] and the direct calculations of the response showing a general absence of superfluidity [51]. In Sec. III we derive the mean-field responses in the specific regime where the spectrum is gapless, for both anisotropic and isotropic cases, which are divergent and superfluid, respectively. This is followed by a catastrophe-theoretic analysis of the anisotropic mean-field behavior of the system in Sec. IV, demonstrating the origin of the mean-field response divergences in bifurcations of the order parameter. Then in Sec. V quantum fluctuations of the system are taken into account to show that, despite isotropic mean-field calculations yielding a superfluid response, the response in gapless regimes is still divergent. This divergence is analyzed both from the perspective of the infinite-dimensional analog of catastrophe theory, renormalization group theory, and of naive perturbation theory, showing that it originates from the phase transitions in these regimes. In Sec. VI we conclude that, as of now, there appear to be no regimes of coherently driven microcavity polaritons that exhibit superfluidity.

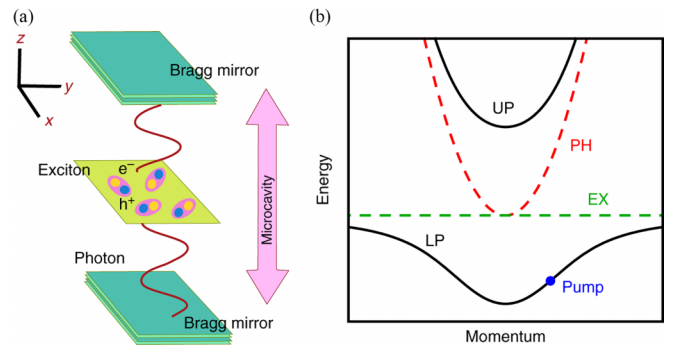


FIG. 1. Polaritons in semiconductor microcavities; figure from [51]. (a) Polaritons are quasiparticles formed when cavity photons, which are massive due to confinement in the  $z$  direction between two Bragg mirrors, interact strongly with excitons confined in a quantum well. Polaritons are free to move in the two-dimensional plane perpendicular to their confinement. (b) The excitonic dispersion (dashed green) is approximately constant compared to the photonic (dashed red) due to the much larger exciton mass. Strong coupling leads to anticrossing and the formation of upper and lower polariton branches (solid black). Polaritons interact because of their excitonic component, while their photonic part causes decay and the need for an external drive. A coherent laser pump resonantly tuned to the polariton dispersion is marked by a blue dot.

## II. PRIOR ART: COHERENTLY DRIVEN MICROCAVITY POLARITONS AND THE QUESTION OF SUPERFLUIDITY

The present paper seeks to answer questions related to superfluidity in coherently driven microcavity polaritons, raised by some special regimes not addressed in the general treatment by [51]. This section is thus devoted to a summary of relevant theoretical work in this field and an introduction to the specific regimes of interest.

### A. Strong coupling of photons and excitons: The coherently driven lower polariton model

Semiconductor microcavities are typically constructed by placing semiconductor quantum wells supporting Wannier-Mott excitons between Bragg reflectors (layers of alternating refractive index material leading to high-quality reflection for wavelengths close to four times the layer widths), typically spaced microns apart [Fig. 1(a)]. Semiconductor quantum wells are thin layers of semiconductor with a thickness comparable to the exciton Bohr radius, sandwiched between two barrier layers with a much larger band gap. The exciton center-of-mass motion is quantized in the confinement direction, and the wells are typically engineered to support only the lowest of these energy modes at the relevant energies, making the excitons quasi-2D particles [12].

Photons trapped in the cavity also behave as quasi-2D particles, developing an effective mass related to their quantized mode in the confinement direction. Typically only the lowest mode is considered, and the effective energy spectrum becomes

$$\omega_c(\mathbf{k}) = \frac{c}{n} \sqrt{\left(\frac{2\pi}{L_w}\right)^2 + k^2}, \quad (1)$$

where  $n$  is the refractive index of the quantum well and  $L_w$  is the cavity width.

With appropriate tuning, the system can be described by a Jaynes-Cummings interaction:

$$H_0 = \sum_{\mathbf{k}} \omega_c(\mathbf{k}) c_{\mathbf{k}}^\dagger c_{\mathbf{k}} + \sum_{\mathbf{k}} \omega_x(\mathbf{k}) x_{\mathbf{k}}^\dagger x_{\mathbf{k}} + \frac{\Omega_R}{2} \sum_{\mathbf{k}} (c_{\mathbf{k}}^\dagger x_{\mathbf{k}} + x_{\mathbf{k}}^\dagger c_{\mathbf{k}}) \quad (2)$$

with quasi-2D photon annihilation operators  $c_{\mathbf{k}}$  and exciton annihilation operators  $x_{\mathbf{k}}$ , where the Rabi frequency  $\Omega_R$  acts as the exciton-photon coupling constant. In the strong-coupling regime, the Hamiltonian may be approximately diagonalized into quasiparticles known as lower and upper polaritons:

$$H_0 \approx \sum_{\mathbf{k}} \omega_{LP}(\mathbf{k}) a_{LP,\mathbf{k}}^\dagger a_{LP,\mathbf{k}} + \sum_{\mathbf{k}} \omega_{UP}(\mathbf{k}) a_{UP,\mathbf{k}}^\dagger a_{UP,\mathbf{k}} \quad (3)$$

with [Fig. 1(b)]

$$\omega_{UP/LP}(\mathbf{k}) = \frac{1}{2} (\omega_x - \omega_c(\mathbf{k}) \pm \sqrt{[\omega_x - \omega_c(\mathbf{k})]^2 + \Omega_R^2}). \quad (4)$$

The gap between the lower and upper polariton spectra is typically large enough for the lower polaritons to be considered in isolation (from now on we write  $a_{\mathbf{k}}$  for  $a_{LP,\mathbf{k}}$ ) if the relevant energy scales are tuned to them, and excitonic interactions may be modelled as weak contact interactions between polaritons:

$$H_{\text{int}} = \frac{V}{2} \sum_{\mathbf{k}, \mathbf{k}', \mathbf{q}} a_{\mathbf{k}-\mathbf{q}}^\dagger a_{\mathbf{k}'+\mathbf{q}}^\dagger a_{\mathbf{k}} a_{\mathbf{k}'}. \quad (5)$$

Note that this form for the interaction is valid only so long as we may ignore the spatial extent of the excitons. With a typical exciton Bohr radius as high as  $100 \text{ \AA}$ , we must impose a momentum cutoff on our theory of  $k_{\text{max}} = \frac{\hbar}{100 \text{ \AA}}$ . This will also be relevant to our approximations in Appendix A 2. Finally, the system is typically driven-dissipative, meaning that it is externally pumped by a laser and is in contact with a photonic decay bath. Denoting the bath photon modes by  $A_{\mathbf{k}}$  and their

spectrum by  $\omega_A(\mathbf{k})$ , the decay term may be written as

$$H_{\text{bath}} = \sum_{\mathbf{k}} \omega_A(\mathbf{k}) A_{\mathbf{k}}^\dagger A_{\mathbf{k}} + \sum_{\mathbf{k}, \mathbf{q}} \zeta_{\mathbf{k}, \mathbf{q}} (a_{\mathbf{k}}^\dagger A_{\mathbf{q}} + A_{\mathbf{q}}^\dagger a_{\mathbf{k}}). \quad (6)$$

The pump laser is typically applied at some angle to the cavity, leading to an effective pump wave vector  $k_p$  in the cavity plane. A classical coherent pump term, by which we mean resonant or near-resonant with the lower polariton dispersion, may then be represented as

$$H_{\text{pump}} = F_p(t) a_{\mathbf{k}_p}^\dagger + F_p^*(t) a_{\mathbf{k}_p}, \quad (7)$$

where  $F_p(t) = F_p e^{-i\omega_p t}$ , and the implications of neglecting fluctuations in the pump field are discussed in Sec. V B. Performing a gauge transformation  $a \rightarrow a e^{-i\omega_p t}$ , resumming relative to the pump  $\mathbf{k} \rightarrow \mathbf{k} + \mathbf{k}_p$ , and writing  $a_{\mathbf{k}}$  for  $a_{\mathbf{k}+\mathbf{k}_p}$ , the complete Hamiltonian then reads

$$H = \sum_{\mathbf{k}} (\omega_{LP}(\mathbf{k} + \mathbf{k}_p) - \omega_p) a_{\mathbf{k}}^\dagger a_{\mathbf{k}} + \frac{V}{2} \sum_{\mathbf{k}, \mathbf{k}', \mathbf{q}} a_{\mathbf{k}-\mathbf{q}}^\dagger a_{\mathbf{k}'+\mathbf{q}}^\dagger a_{\mathbf{k}} a_{\mathbf{k}'} + \sum_{\mathbf{k}} \omega_A(\mathbf{p} + \mathbf{k}_p) A_{\mathbf{p}}^\dagger A_{\mathbf{p}} + \sum_{\mathbf{k}, \mathbf{p}} \zeta_{\mathbf{k}, \mathbf{p}} (e^{i\omega_p t} a_{\mathbf{k}}^\dagger A_{\mathbf{p}} + A_{\mathbf{p}}^\dagger a_{\mathbf{k}} e^{-i\omega_p t}) + F_p (a_0^\dagger + a_0). \quad (8)$$

Note that this is not a closed-system Hamiltonian, since it incorporates a number nonconserving interaction with laser degrees of freedom the dynamics of which we do not incorporate in the model; rather it is the effective Hamiltonian for the polariton and photon bath subsystem.

## B. Keldysh effective action

In order to work with the above Hamiltonian, it is convenient to eliminate the bath degrees of freedom and obtain an effective action for the polaritons; all questions we wish to ask of the system pertain exclusively to them. This may be achieved by use of the Keldysh path integral technique [52], and this is done in Appendix A. The result is the following effective action in terms of two fields  $\psi^c, \psi^q$ :

$$\mathcal{S}_{\text{eff}} = \sum_{\mathbf{k}} (\bar{\psi}_{\mathbf{k}}^c \quad \bar{\psi}_{\mathbf{k}}^q) \begin{pmatrix} 0 & g^{-1}(k) \\ (g^{-1})^*(k) & 2i\kappa \end{pmatrix} \begin{pmatrix} \psi_{\mathbf{k}}^c \\ \psi_{\mathbf{k}}^q \end{pmatrix} - \frac{V}{2} \sum_{\mathbf{k}, \mathbf{k}', \mathbf{q}} (\bar{\psi}_{\mathbf{k}-\mathbf{q}}^c \bar{\psi}_{\mathbf{k}'+\mathbf{q}}^q [\psi_{\mathbf{k}}^c \psi_{\mathbf{k}'}^c + \psi_{\mathbf{k}}^q \psi_{\mathbf{k}'}^q] + \text{c.c.}) - \sqrt{2} F_p (\bar{\psi}_0^q + \psi_0^q), \quad (9)$$

where  $\Delta_p = \omega_p - \omega_{LP}(0)$ ,  $g^{-1}(k) = \omega + \Delta_p - \epsilon(\mathbf{k}) - i\kappa$ ,  $\kappa$  is a constant related to the system's dissipation, and  $\omega_{LP}(\mathbf{k} + \mathbf{k}_p) - \omega_{LP}(0) = \epsilon(\mathbf{k})$ . Note that unbolded momentum variables are 4-vectors, standing for the combination of frequency and momentum as  $k = (\omega, \mathbf{k})$ .

In the absence of the last term,  $\sqrt{2} F_p (\bar{\psi}_0^q + \psi_0^q)$ , the action possesses a global  $U(1)$  symmetry  $\psi_k^{c/q} \rightarrow \psi_k^{c/q} e^{i\theta}$ . Such symmetry in condensed matter systems is often indicative of superfluidity [39], and incoherently pumped systems can indeed be shown to exhibit it [31]. The drive term, however, breaks the  $U(1)$  symmetry, since the phase of the pump  $F_p$  is independent of that of the fields.

The mean-field equations for this action are found by functional differentiation to be

$$\frac{d\mathcal{S}_{\text{eff}}}{d\bar{\psi}^c(k)} = [\omega + \Delta_p - \epsilon(\mathbf{k}) - i\kappa] \psi^q(k) - \frac{V}{2} \sum_{\mathbf{k}', \mathbf{q}} (\bar{\psi}^q(k' + \mathbf{q}) [\psi^c(k + \mathbf{q}) \psi^c(k') + \psi^q(k + \mathbf{q}) \psi^q(k')]) + 2\bar{\psi}^c(k' + \mathbf{q}) \psi^q(k + \mathbf{q}) \psi^c(k') = 0, \quad (10)$$

$$\begin{aligned} \frac{d\mathcal{S}_{\text{eff}}}{d\psi^c(-k)} &= [-\omega + \Delta_p - \epsilon(-\mathbf{k}) + i\kappa]\bar{\psi}^q(-k) - \frac{V}{2} \sum_{k',q} (\psi^q(k' + q)[\bar{\psi}^c(-k + q)\bar{\psi}^c(k') + \bar{\psi}^q(-k + q)\bar{\psi}^q(k')] \\ &\quad + 2\psi^c(k' + q)\bar{\psi}^q(-k + q)\bar{\psi}^c(k') = 0, \end{aligned} \quad (11)$$

$$\begin{aligned} \frac{d\mathcal{S}_{\text{eff}}}{d\bar{\psi}^q(k)} &= [\omega + \Delta_p - \epsilon(\mathbf{k}) + i\kappa]\psi^c(k) - \frac{V}{2} \sum_{k',q} (\bar{\psi}^c(k' + q)[\psi^c(k + q)\psi^c(k') + \psi^q(k + q)\psi^q(k')] \\ &\quad + 2\bar{\psi}^q(k' + q)\psi^q(k + q)\psi^c(k') + 2i\kappa\psi^q(k) - \sqrt{2}F_p\delta_{k,0} = 0, \end{aligned} \quad (12)$$

$$\begin{aligned} \frac{d\mathcal{S}_{\text{eff}}}{d\psi^q(-k)} &= [-\omega + \Delta_p - \epsilon(-\mathbf{k}) - i\kappa]\bar{\psi}^c(-k) - \frac{V}{2} \sum_{k',q} (\psi^c(k' + q)[\bar{\psi}^c(-k + q)\bar{\psi}^c(k') + \bar{\psi}^q(-k + q)\bar{\psi}^q(k')] \\ &\quad + 2\psi^q(k' + q)\bar{\psi}^q(-k + q)\bar{\psi}^c(k') + 2i\kappa\bar{\psi}^q(-k) - \sqrt{2}F_p\delta_{-k,0} = 0. \end{aligned} \quad (13)$$

Assuming the solution to be space-time homogeneous and classical ( $\psi^c(k) = \sqrt{2}\psi_0\delta_{k,0}$ ,  $\psi^q(k) = 0$ ), the equations simplify to

$$[\Delta_p - \epsilon(\mathbf{0}) + i\kappa]\psi_0 - F_p = V|\psi_0|^2\psi_0, \quad (14)$$

$$[\Delta_p - \epsilon(\mathbf{0}) - i\kappa]\bar{\psi}_0 - F_p = V|\psi_0|^2\bar{\psi}_0. \quad (15)$$

Writing  $\delta_p = \Delta_p - \epsilon(\mathbf{0})$  for the detuning, mod-squaring the above yields a cubic equation for the mean-field occupancy of the pump mode  $n = |\psi_0|^2$ :

$$V^2n^3 - 2\delta_pVn^2 + (\delta_p^2 + \kappa^2)n - F_p^2 = 0. \quad (16)$$

Depending on whether  $\delta_p > \sqrt{3}\kappa$  or  $\delta_p \leq \sqrt{3}\kappa$ , the equation may or may not have multiple (specifically, three) real solutions for certain values of  $F_p$ . The former case is referred to as the bistable regime and will be of primary interest to us in this paper.

For a particular value of  $\psi_0$ , the action may be rewritten via the background field method in terms of the fields  $\psi^c(k) \rightarrow \psi^c(k) - \psi_0\delta_{k,0}$ ,  $\psi^q(k) \rightarrow \psi^q(k)$ . Up to second order in the fields this yields

$$\mathcal{S}_{\text{eff}} = \mathcal{S}_{\text{eff}}|_{\psi=\psi_0} + \frac{1}{2} \sum_{k,k'} \Psi^\dagger(k) \mathcal{D}^{-1}(k, k') \Psi(k') + O(\psi^3), \quad (17)$$

where

$$\mathcal{D}^{-1}(k, k') = \begin{pmatrix} 0 & 0 & J^*(k) & -V\psi_0^2 \\ 0 & 0 & -V\bar{\psi}_0^2 & J(-k) \\ J(k) & -V\psi_0^2 & 2i\kappa & 0 \\ -V\bar{\psi}_0^2 & J^*(-k) & 0 & 2i\kappa \end{pmatrix} \delta_{k,k'} \quad (18)$$

and  $J(k) = \omega + \Delta_p - \epsilon(\mathbf{k}) + i\kappa - 2V|\psi_0|^2$ . Here we have written the action in terms of the Nambu vector  $\Psi(k) = (\psi^c(k), \bar{\psi}^c(-k), \psi^q(k), \bar{\psi}^q(-k))$ . This introduces a measure of redundancy to the expression which is explained in detail in Appendix B, where the corresponding diagrammatics are also worked out. Taking this into account, the bare propagators are

given in terms of the block matrix

$$\begin{pmatrix} i\underline{G}_K(k, k') & i\underline{G}_R(k, k') \\ i\underline{G}_A(k, k') & \underline{0} \end{pmatrix} = \mathcal{D}(k, k'), \quad (19)$$

where the blocks are  $2 \times 2$  matrices in Nambu space. Each block is named for its corresponding top left entry, so that the conventional Keldysh Green's functions are given by  $G_{K/R/A}(k, k') = (\underline{G}_{K/R/A}(k, k'))^{11}$ . The exact expressions for these are given in the Appendixes, and in the next section we will use them to study the system spectrum.

### C. System spectrum and the Landau criterion

One of the oldest criteria by which the superfluidity of a system may be judged is due to Landau [39] and relies entirely on the system's quasiparticle excitation spectrum  $\epsilon(\mathbf{p})$ . Consider a fluid with total mass  $M$  moving with velocity  $\mathbf{V}$  in the laboratory frame. Suppose now that, through interaction with some external perturbation (e.g., a capillary wall or substrate defect), a quasiparticle with momentum  $\mathbf{p}$  is created. By conservation of momentum

$$M\mathbf{V} = M\mathbf{V}' + \mathbf{p}, \quad (20)$$

where  $\mathbf{V}'$  is the new velocity, and thus the new total energy is

$$E' = \frac{1}{2}MV'^2 + \epsilon(\mathbf{p}) = \frac{1}{2}MV^2 + \epsilon(\mathbf{p}) - \mathbf{V} \cdot \mathbf{p} + \frac{p^2}{2M}. \quad (21)$$

For large  $M$  the last term may be neglected, and we see that for the system to lose energy via dissipation we must have

$$\min_{\mathbf{p}} [\epsilon(\mathbf{p}) - \mathbf{V} \cdot \mathbf{p}] < 0. \quad (22)$$

For an isotropic system this is equivalent to  $\min_p[\epsilon(p) - Vp] < 0$ , and the largest value of  $V$  for which this does not hold  $V_{\text{crit}} = \min_p \frac{\epsilon(p)}{p}$  is termed the critical velocity. This is because for fluid velocities not exceeding this value, it is energetically unfavorable for the system to generate excitations and thus the system cannot dissipate energy via this route—non-dissipative flow characteristic of a superfluid occurs.

The Landau criterion is not rigorously applicable to driven-dissipative systems. It assumes a real excitation spectrum, which in such systems is generally complex, and relies on a conservation of energy argument that may be violated by

the external drive. Nevertheless, some works have presented results via a heuristic application of it to the real part of the complex spectrum of coherently driven exciton-polaritons in the bistable regime [11,49,50].

The excitation spectrum of the system may be obtained from the poles of the retarded Green's function [53], which is given by (see Appendix B):

$$G_R(k) = \frac{J^*(-k)}{J(k)J^*(-k) - V^2|\psi_0|^4}. \quad (23)$$

The spectrum  $\omega(\mathbf{k})$  is thus given by the solution to

$$J(\omega(\mathbf{k}), \mathbf{k})J^*(-\omega(\mathbf{k}), -\mathbf{k}) - V^2|\psi_0|^4 = 0 \quad (24)$$

and is found to be

$$\omega^\pm(\mathbf{k}) = \frac{\epsilon(\mathbf{k}) - \epsilon(-\mathbf{k})}{2} - i\kappa \pm \sqrt{\left(\frac{\epsilon(\mathbf{k}) + \epsilon(-\mathbf{k})}{2} - \Delta_p + 2V|\psi_0|^2\right)^2 - V^2|\psi_0|^4}. \quad (25)$$

For  $\mathbf{k}_p = 0$ ,  $\text{Re } \omega^+(\mathbf{k}) = -\text{Re } \omega^-(\mathbf{k})$ ,  $\text{Im } \omega^+(\mathbf{k}) = \text{Im } \omega^-(\mathbf{k})$ , and the  $\omega^-(\mathbf{k})$  negative energy branch corresponds to the same physical excitations as the positive energy one. It may thus be interpreted as the spectrum for ‘‘holes’’ and is sometimes referred to as the ghost branch.

For  $\mathbf{k}_p \neq 0$ , due to our resummation with respect to the pump momentum in (8), we may view the system's action as that for an isotropically pumped (and thus stationary) fluid of polaritons but with a tilted energy spectrum. While similar to a change of reference frame to one in which the polaritons are stationary, we emphasize that this is simply a formal manipulation of the action. Writing  $\epsilon(\mathbf{k}) \approx \frac{(\mathbf{k} + \mathbf{k}_p)^2}{2m}$  where  $m$  is the effective polariton mass, to linear order one finds that

$$\omega^\pm(\mathbf{k}) = \omega^\pm(\mathbf{k})|_{\mathbf{k}_p=0} + \frac{\mathbf{k}_p}{m} \cdot \mathbf{k} + O(|\mathbf{k}_p|^2), \quad (26)$$

which shows that the tilt is due to the bulk flow of the fluid (induced by the pump) with velocity  $\mathbf{v} = \frac{\hbar\mathbf{k}_p}{m}$ . From this point of view, superfluidity will be destroyed when the linear tilt becomes so significant as to push  $\omega^\pm(\mathbf{k})$  for some nonzero  $k$  below the energy of the condensed mode  $\omega^\pm(0)$  so that particles may scatter into this new mode. Comparing with (22), it is evident that this is equivalent to applying the Landau criterion to the real part of the spectrum without this linear correction [here  $\delta_p = \Delta_p - \epsilon(0)$ ]:

$$\begin{aligned} \text{Re } \omega_{\text{rest}}^+(\mathbf{k}) \\ = \text{Re } \sqrt{(\epsilon(\mathbf{k})|_{\mathbf{k}_p=0} - \delta_p + 2V|\psi_0|^2)^2 - V^2|\psi_0|^4}. \end{aligned} \quad (27)$$

Here three situations are possible. If  $V|\psi_0|^2 < \delta_p$  then, for some value of  $|\mathbf{k}_0| \neq 0$ ,

$$\epsilon(\mathbf{k}_0)|_{\mathbf{k}_p=0} - \delta_p + 2V|\psi_0|^2 = 0 \quad (28)$$

and  $\text{Re } \omega^+(\mathbf{k}_0)|_{\mathbf{k}_p=0} = 0$ , meaning the critical velocity is zero and there is no superfluid (per the Landau criterion). If  $V|\psi_0|^2 > \delta_p$ , then the spectrum is gapped and there is a positive critical velocity and associated superfluidity. This velocity

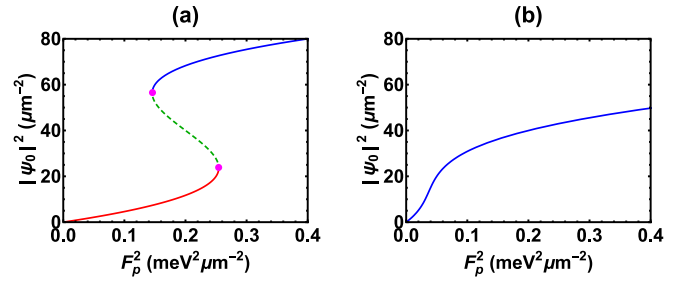


FIG. 2. Absolute value squared of the homogeneous solution  $\psi_0$  to the mean-field equations for varying values of the pump  $F_p$ . The left figure corresponds to the  $\delta_p = 3\kappa > \sqrt{3}\kappa$  bistable regime with multivalued solutions and inversion points (marked by fuchsia dots), while the right corresponds to the monostable  $\delta_p < \sqrt{3}\kappa$  regime with a single solution for each pump value.

is given by

$$\begin{aligned} V_{\text{crit}} \\ = \sqrt{\frac{-\delta_p + 2V|\psi_0|^2 - \sqrt{(-\delta_p + 2V|\psi_0|^2)^2 - V^2|\psi_0|^4}}{m}}. \end{aligned} \quad (29)$$

Finally, if  $V|\psi_0|^2 = \delta_p$ , then the real spectrum is gapless at  $|\mathbf{k}| = 0$  and its gradient there (the polariton ‘‘sound velocity’’) must be considered. This derivative comes out as

$$V_{\text{crit}} = \left. \frac{d \text{Re } \omega_{\text{rest}}^+(|\mathbf{k}|)}{d|\mathbf{k}|} \right|_{\mathbf{k}=0} = \sqrt{\frac{V|\psi_0|^2}{m}}, \quad (30)$$

which agrees with the limit of the previous expression in  $\delta_p$ .

This discussion can be specialized to the case of the bistable regime, where the mean-field solution of Eq. (16) can be split into three branches (red, green, and blue in Fig. 2). These branches are separated by points called ‘‘inversion points,’’ which correspond to

$$V|\psi_0|^2 = \frac{1}{3}(2\delta_p \pm \sqrt{\delta_p^2 - 3\kappa^2}). \quad (31)$$

We thus see that  $V|\psi_0|^2 < \delta_p$  on the lower red branch, and so superfluidity cannot occur there per the Landau criterion. The middle green branch can be shown to be dynamically unstable since

$$\exists \mathbf{k} \text{ s.t. } \text{Im } \omega^\pm(\mathbf{k}) > 0 \quad (32)$$

for every point on that branch (a simple proof of this is given in Sec. IV A), and this is an indication of dynamical instability [53]. Thus, according to the Landau criterion, superfluidity is present on the upper blue branch for every point with  $V|\psi_0|^2 \geq \delta_p$ .

## D. Current-current response and the rigid state

### 1. Linear-response superfluid criterion

Because of the aforementioned heuristic nature of the Landau criterion when applied to driven-dissipative systems, however, the work on which we are building [51] opted to use a linear response-based criterion [39,40], one which has even been proposed as a generalized definition of a superfluid [11].

The results, which we briefly outline now, partially differ from the Landau criterion analysis and highlight its limitations in a driven-dissipative context.

For a system possessing a conserved current  $j(\mathbf{x}, t)$ , consider a Hamiltonian perturbation of the form

$$- \int d\mathbf{x} dt \mathbf{j}(\mathbf{x}, t) \cdot \mathbf{u}(\mathbf{x}, t), \quad (33)$$

where  $\mathbf{u}(\mathbf{x}, t)$  is an external field. Considering the historical example of fluid in a capillary, this generalizes the term  $-m \int d\mathbf{x} dt \mathbf{j}(\mathbf{x}, t) \cdot \mathbf{u}(t) = -\mathbf{P} \cdot \mathbf{u}(t)$ , which appears in the superfluid's rest frame Hamiltonian when the walls are moving with velocity  $\mathbf{u}(t)$ . The Helmholtz decomposition of  $\mathbf{u}(\mathbf{x}, t)$ ,

$$\mathbf{u}(\mathbf{x}, t) = \underbrace{-\nabla \Phi(\mathbf{x}, t)}_{\text{longitudinal}} + \underbrace{\nabla \times \mathbf{A}(\mathbf{x}, t)}_{\text{transverse}}, \quad (34)$$

consists of longitudinal and transverse components. Intuitively, the gradient term corresponds to some sort of push, while the curl term introduces shear. The generalization of the classical superfluid's frictionless flow through a capillary is the statement that its current does not respond to transverse perturbations, since friction with the walls is a shearing force.

To study this (linear) response, we require the current-current response tensor. By Kubo's formula, this is

$$\chi_{ij}(\mathbf{x}, t, \mathbf{x}', t') = i\theta(t - t') \langle [j_i(\mathbf{x}, t), j_j(\mathbf{x}', t')] \rangle. \quad (35)$$

In an isotropic, time and space translation-invariant system, the most general form the static ( $\omega = 0$ ) Fourier transform of this quantity can take is

$$\chi_{ij}(\mathbf{k}) = \frac{k_i k_j}{k^2} \chi_L(k) + \left( \delta_{ij} - \frac{k_i k_j}{k^2} \right) \chi_T(k). \quad (36)$$

The subscripts indicate that the first term couples to the longitudinal component of the static Helmholtz decomposition,  $-\mathbf{k}\Phi(\mathbf{k})$ , while the second couples to the transverse component  $\mathbf{k} \times \mathbf{A}(\mathbf{k})$ . Using the special form of (36), we observe that the static limits of the normal and transverse components may be extracted by sequential limits. For example,

$$\lim_{k_y \rightarrow 0} \lim_{k_x \rightarrow 0} \chi_{xx} = \lim_{k \rightarrow 0} \chi_T(k), \quad (37)$$

$$\lim_{k_x \rightarrow 0} \lim_{k_y \rightarrow 0} \chi_{xx} = \lim_{k \rightarrow 0} \chi_L(k). \quad (38)$$

While we will use this property later to perform explicit calculations, it is worth highlighting what it suggests about the response tensor. Namely, in order for a system to possess different transverse and longitudinal responses, the response tensor must be discontinuous at zero momentum. Superfluidity is then defined in the thermodynamic limit as a difference between the static, homogeneous linear, and transverse responses:

$$\lim_{k \rightarrow 0} (\chi_L(k) - \chi_T(k)) > 0 \Rightarrow \text{superfluid}. \quad (39)$$

While this response tensor should be calculated in the superfluid's rest frame, it is sometimes instructive to examine its behavior in other frames [though it may no longer take the form (36)]. We will see this to be the case when we study the case  $\mathbf{k}_p \neq 0$  later.

## 2. Nonequilibrium current

The above definition relies on a conserved system current, but the situation is more complicated for driven-dissipative systems. For such systems, we are interested in the component of the current that is internal to the system as opposed to the component relating to pump and dissipation. This is known as the coherent current [54] and takes the familiar form

$$\mathbf{j}(\mathbf{x}, t) = \frac{1}{2mi} (\bar{\psi} \nabla \psi - \psi \nabla \bar{\psi}). \quad (40)$$

In [51] care is taken to normal-order this operator. Normal ordering, however, affects only the expectation of the operator up to a constant. Since we are interested in the linear response of this expectation the constant is irrelevant.

Suppose that we introduce a term of the form

$$- \int d\mathbf{x} dt \mathbf{j}(\mathbf{x}, t) \cdot \mathbf{u}(\mathbf{x}, t) \quad (41)$$

to the original Hamiltonian, where  $\mathbf{u}$  is a classical field. Writing  $\mathbf{j}^+$  for (40) written in terms of fields on the forward contour, and similarly  $\mathbf{j}^-$  for the backward contour, this will give the following contribution to the overall Keldysh action:

$$\int d\mathbf{x} dt (\mathbf{j}^+(\mathbf{x}, t) \cdot \mathbf{u}^+(\mathbf{x}, t) - \mathbf{j}^-(\mathbf{x}, t) \cdot \mathbf{u}^-(\mathbf{x}, t)). \quad (42)$$

We may now define, by analogy with the classical and quantum fields, the classical and quantum current operators  $\mathbf{j}^c, \mathbf{j}^q$  as

$$\mathbf{j}^c = \frac{1}{2} (\mathbf{j}^+ + \mathbf{j}^-), \quad (43)$$

$$\mathbf{j}^q = (\mathbf{j}^+ - \mathbf{j}^-). \quad (44)$$

Also introducing the "physical" field  $\mathbf{f} = \frac{1}{2} (\mathbf{u}^+ + \mathbf{u}^-)$  and the "unphysical" field  $\boldsymbol{\theta} = \mathbf{u}^+ - \mathbf{u}^-$ , the significance of which will be explained shortly, we may rewrite (42) as

$$\int d\mathbf{x} dt (\mathbf{j}^c(\mathbf{x}, t) \cdot \boldsymbol{\theta}(\mathbf{x}, t) + \mathbf{j}^q(\mathbf{x}, t) \cdot \mathbf{f}(\mathbf{x}, t)). \quad (45)$$

Since the classical field is the same on both contours,  $\mathbf{u}^+ = \mathbf{u}^-$ , we have that the unphysical field  $\boldsymbol{\theta} = 0$ , which motivates its name. On the other hand the physical field is equal to the original field  $\mathbf{f} = \mathbf{u}$ . The perturbation to the Keldysh action thus takes the form

$$\int d\mathbf{x} dt \mathbf{j}^q(\mathbf{x}, t) \cdot \mathbf{f}(\mathbf{x}, t), \quad (46)$$

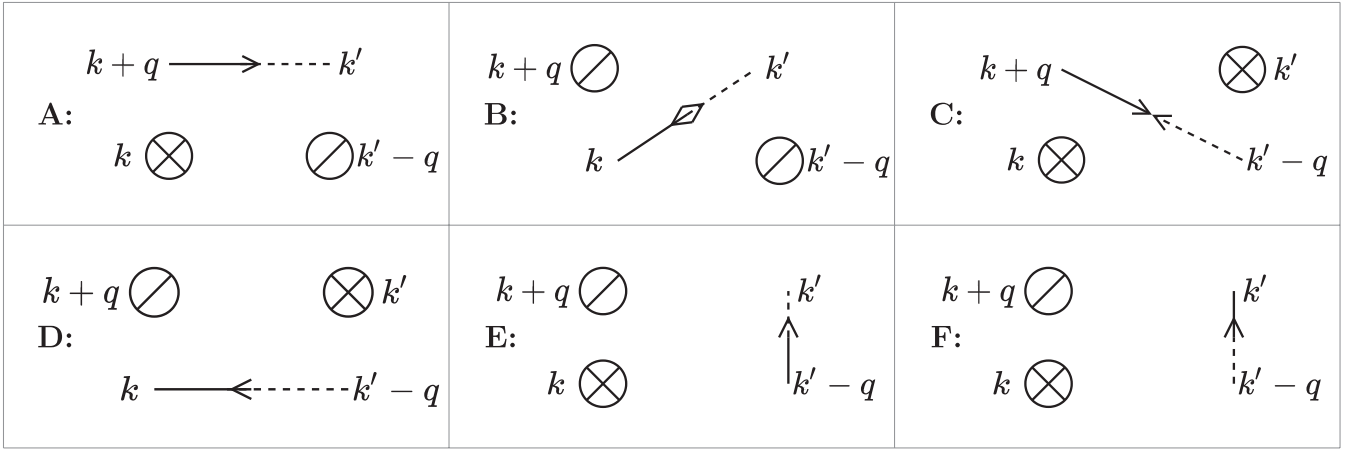
from which one can see that the first perturbative correction to the expectation of the classical current will be

$$\int d\mathbf{x}' dt' i \langle \mathbf{j}^c(\mathbf{x}, t) \mathbf{j}^q(\mathbf{x}', t') \rangle \cdot \mathbf{f}(\mathbf{x}', t'). \quad (47)$$

Since, up to normal ordering, the expectation value of the classical current is equal to the expectation value of the true current, this shows that the response function we seek is given by

$$\chi_{ij}(\mathbf{x}, t, \mathbf{x}', t') = i \langle j_i^c(\mathbf{x}, t) j_j^q(\mathbf{x}', t') \rangle, \quad (48)$$

and we may view the response we seek as the response of the classical current to the physical field. This result is derived in an alternative way in [54].


 FIG. 3. Order  $O(\hbar)$  diagrams for the current-current response.

In terms of Fourier-transformed fields, (46) is

$$\sum_{\mathbf{k}} \mathbf{j}^q(-\mathbf{k}) \cdot \mathbf{f}(\mathbf{k}) \quad (49)$$

so that the static response in terms of these fields becomes

$$\chi_{ij}(0, \mathbf{q}) = \chi_{ij}(\mathbf{q}) = \frac{i}{2} \langle j_i^c(0, \mathbf{q}) j_j^q(0, -\mathbf{q}) \rangle, \quad (50)$$

while the static classical and quantum currents are given by

$$i^c(0, \mathbf{q}) = j_i^c(\mathbf{q}) \quad (51)$$

$$= \sum_{\omega, \mathbf{k}} \gamma_i(2\mathbf{k} + \mathbf{q}) [\psi^c(\omega, \mathbf{k} + \mathbf{q}) \bar{\psi}^c(\omega, \mathbf{k})] \quad (52)$$

$$+ \psi^q(\omega, \mathbf{k} + \mathbf{q}) \bar{\psi}^q(\omega, \mathbf{k}), \quad (53)$$

$$i^q(0, \mathbf{q}) = j_i^q(\mathbf{q}) \quad (54)$$

$$= \sum_{\omega, \mathbf{k}} \gamma_i(2\mathbf{k} + \mathbf{q}) [\psi^c(\omega, \mathbf{k} + \mathbf{q}) \bar{\psi}^q(\omega, \mathbf{k})] \quad (55)$$

$$+ \psi^q(\omega, \mathbf{k} + \mathbf{q}) \bar{\psi}^c(\omega, \mathbf{k}), \quad (56)$$

where  $\gamma(\mathbf{q}) = \frac{\mathbf{q} + \mathbf{k}_p}{2m}$ .

### 3. The rigid state

The response tensor may be worked out perturbatively using the diagrammatics of Appendix B. At order  $O(\hbar)$  there are six diagrams, presented in Fig. 3. Placing one current operator on the left of the diagram and one on the right, the first four of

these come out to

$$\begin{aligned} & -|\psi_0|^2 G_R^{11}(0, \mathbf{q}) \gamma_i(\mathbf{q}) \gamma_j(\mathbf{q}) - \psi_0^2 G_R^{21}(0, \mathbf{q}) \gamma_i(-\mathbf{q}) \gamma_j(\mathbf{q}) \\ & - \bar{\psi}_0^2 G_R^{12}(0, \mathbf{q}) \gamma_i(\mathbf{q}) \gamma_j(-\mathbf{q}) - |\psi_0|^2 G_R^{22}(0, \mathbf{q}) \gamma_i(-\mathbf{q}) \gamma_j(-\mathbf{q}), \end{aligned} \quad (57)$$

while the last two yield the more complicated term

$$-\gamma_i(0) |\psi_0|^2 \delta_{\mathbf{q},0} \sum_{\omega', \mathbf{k}'} [G_R^{11}(\omega', \mathbf{k}') + G_A^{11}(\omega', \mathbf{k}')] \gamma_j(2\mathbf{k}'). \quad (58)$$

This term is zero by the Keldysh identity  $\sum_{\omega} [G_R^{11}(\omega, \mathbf{k}) + G_A^{11}(\omega, \mathbf{k})] = 0$ , so at order  $O(\hbar)$  the current-current response is given by

$$\begin{aligned} \chi_{h,ij}(\mathbf{q}) = & -|\psi_0|^2 G_R^{11}(0, \mathbf{q}) \gamma_i(\mathbf{q}) \gamma_j(\mathbf{q}) \\ & - \psi_0^2 G_R^{21}(0, \mathbf{q}) \gamma_i(-\mathbf{q}) \gamma_j(\mathbf{q}) \\ & - \bar{\psi}_0^2 G_R^{12}(0, \mathbf{q}) \gamma_i(\mathbf{q}) \gamma_j(-\mathbf{q}) \\ & - |\psi_0|^2 G_R^{22}(0, \mathbf{q}) \gamma_i(-\mathbf{q}) \gamma_j(-\mathbf{q}). \end{aligned} \quad (59)$$

We may briefly comment on the physical significance of these diagrams, as related in [31] (the present diagrams correspond to the first diagram in Fig. 1 of that paper). In all (nonzero) of these, each current vertex scatters a particle out of the condensate and thus yields a term of the form  $\gamma_i(\mathbf{q})$ . All such diagrams thus contribute to the superfluid  $q_i q_j$  component of the response tensor.

We may expand this expression out to facilitate taking appropriate limits. Substituting in for the propagators and splitting  $\gamma_i(\mathbf{q}) = \frac{1}{2m}(\mathbf{q})_i + \frac{1}{2m}(\mathbf{k}_p)_i$  yields

$$\begin{aligned} \chi_{h,ij}(\mathbf{q}) = & -\frac{|\psi_0|^2}{4m^2(J(\mathbf{q})J^*(-\mathbf{q}) - V^2|\psi_0|^4)} ([J(\mathbf{q}) + J^*(-\mathbf{q}) + 2V|\psi_0|^2](\mathbf{k}_p)_i(\mathbf{k}_p)_j - [J(\mathbf{q}) - J^*(-\mathbf{q})](\mathbf{q})_i(\mathbf{k}_p)_j \\ & - [J(\mathbf{q}) - J^*(-\mathbf{q})](\mathbf{k}_p)_i(\mathbf{q})_j + [J(\mathbf{q}) + J^*(-\mathbf{q}) - 2V|\psi_0|^2](\mathbf{q})_i(\mathbf{q})_j). \end{aligned} \quad (60)$$

So long as  $J(\mathbf{0})J^*(-\mathbf{0}) - V^2|\psi_0|^4 \neq 0$  (the condition for the complex spectrum to be gapped), the  $\mathbf{q} \rightarrow \mathbf{0}$  limit of this quantity is direction-independent and comes out to

$$\chi_{h,ij}(\mathbf{0}) = - \frac{|\psi_0|^2(2\delta_p - 2V|\psi_0|^2)}{4m^2(3V^2|\psi_0|^4 - 4\delta_p V|\psi_0|^2 + \delta_p^2 + \kappa^2)} \times (\mathbf{k}_p)_i(\mathbf{k}_p)_j. \quad (61)$$

This homogeneous response is not in the fluid's rest frame and thus not isotropic unless  $\mathbf{k}_p = 0$ , so the tensor cannot be decomposed as in (36). Note, however, that the direction independence of the limit means that for a perturbation in a given direction  $\mathbf{d}$ , for  $\mathbf{q} \rightarrow 0$  the response is  $\chi_{h,ij}(\mathbf{0})(\mathbf{d}(\mathbf{0}))_j$  and is thus independent of whether the perturbation was longitudinal or transverse. This absence of a discontinuity at  $\mathbf{k} = 0$  will be unaffected by a change of frame, so we may conclude that the response is entirely nonsuperfluid. More specifically, it will be shown in Sec. IV B 2 that it can be interpreted as a change in occupation of the macroscopically occupied  $\mathbf{q} = \mathbf{k}_p$  pump state (also referred to as the condensate, and corresponding to  $\psi_0$  due to the momentum shift performed earlier), so that the homogeneous component of the nonequilibrium current is rigidly in the  $\mathbf{k}_p$  direction. This situation was referred as the system being in a “rigid state” by [51].

A particularly interesting situation occurs when  $V|\psi_0|^2 = \delta_p$ , as the response then vanishes entirely even at  $\mathbf{k}_p \neq 0$ . This corresponds to what is sometimes known as the “sonic point,” as here the real part of the spectrum becomes gapless and linear (refer to Sec. II C) and has been studied in experiments where the polariton fluid was induced to flow past a defect [25]. Such experiments report significantly reduced scattering of the fluid by the defect (also referred to as frictionless flow) in this regime and interpret this as a sign of superfluidity. We argue, however, that what was actually detected was the vanishing of the linear response in its entirety. This means that, while scattering is indeed expected to be reduced, the transverse and longitudinal responses are equal and both zero so that the system is in the unique rigid state rather than a superfluid state: “frictionless flow in the sonic regime is the only property associated with superfluidity that is exhibited by this rigid state, as vortices and persistent currents cannot form when the phase is externally fixed” (note that recent work has demonstrated that the topological defects associated with coherently driven polaritons are domain walls rather than vortices [55]), “and the superfluid response is zero” [51].

A number of groups have also experimentally measured the spectrum in the sonic regime based on a belief in the importance of the linearization of the real part of the spectrum (and thus it taking on a Bogoliubov form) to the Landau criterion [56–58]. Such interest in this point as a superfluid candidate warrants an explanation for why we detect no superfluid response despite the linearized spectrum.

Recall that, in order for a superfluid response to be present, there must be a discontinuity in the current-current response at zero momentum. Yet a crucial effect of the excitation spectrum in Bose-condensed systems in the weakly interacting regime relates to the fact that in such systems the poles of one-particle Green's functions coincide with those of density and current response functions (strictly speaking nonanalyticities of the response functions, since a pole of the Green's function may become “smoothed out” in the response function) [42,59]. This is easily seen to be the case for our system, where the mean-field current-current response is a linear

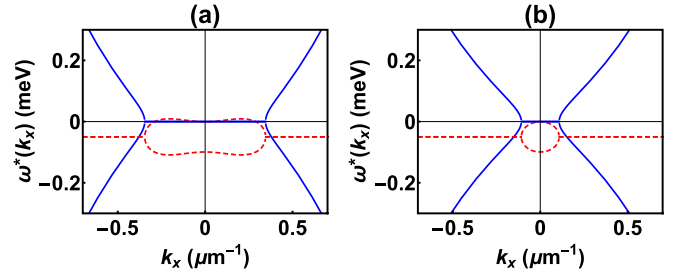


FIG. 4. Gapless excitation spectra at the bistability inversion points, where blue is the real part and dashed-red imaginary, for the isotropic  $k_p = 0$  case. (a) The spectrum at the the inversion point on the lower branch in Fig. 2(a). (b) The spectrum at the the inversion point on the upper branch in Fig. 2(a). For the anisotropic case, where  $k_p \neq 0$ , the real spectra are tilted but still gapless.

combination of the retarded Green's functions [see (59)]. Thus, in order for our static ( $\omega = 0$ ) response to possess a discontinuity at  $\mathbf{k} = 0$ , the retarded Green's functions must possess a pole at  $\omega = 0$ ,  $\mathbf{k} = 0$ . This corresponds to a condition that the spectrum be gapless and, in an equilibrium system with a purely real spectrum, the linearized Bogoliubov spectrum would be. In a driven-dissipative system such as ours, however, the spectrum also possesses an imaginary part, and this is found to be nonzero in the sonic regime (both analytically and from linewidth measurements in the cited experimental papers). Thus a linearized Bogoliubov form of the real part of the spectrum is not a sufficient condition for superfluidity in such systems: this is an important distinction between equilibrium and driven-dissipative systems due to the possibility of complex dispersion relations for the latter.

Overall, it appears that heuristic application of the Landau criterion correctly identifies points at which no superfluid is present; it agrees with the response analysis that no superfluid is present for  $V|\psi_0|^2 < \delta_p$ . Unfortunately it seems to also yield false positives, since it predicts superfluidity for points with  $V|\psi_0|^2 > \delta_p$  (possessing a gapped real spectrum), whereas the linear response at these points is found to be nonsuperfluid. The Landau criterion does correctly identify the frictionless regime  $V|\psi_0|^2 = \delta_p$ , but it appears that this regime lacks not only a transverse but also a longitudinal response and is thus not a conventional superfluid but rather a special case of the rigid state with vanishing linear response and thus reduced friction.

### III. MEAN-FIELD RESPONSE IN THE GAPLESS REGIME

The above analysis was restricted to the case of  $J(\mathbf{0})J^*(-\mathbf{0}) - V^2|\psi_0|^4 \neq 0$ , where the complex spectrum is gapped. At the inversion points, however, this condition fails, which can be seen in Fig. 4.

To investigate how this change in the spectrum affects the response to perturbations of coherently pumped polaritons, we calculate the homogeneous behavior of the mean-field response function [Eq. (60)] in this regime. Assuming a uniformly oriented perturbing field  $\mathbf{u}(\mathbf{q})$ , the longitudinal response can be found by taking the momentum to zero along the direction of the perturbation ( $\mathbf{u} \perp \mathbf{q} = 0$ ,  $\mathbf{u} \parallel \mathbf{q} \rightarrow 0$ ), and analogously for the transverse response ( $\mathbf{u} \parallel \mathbf{q} = 0$ ,  $\mathbf{u} \perp$

$\mathbf{q} \rightarrow 0$ ). To do this, we separate the response function into its numerator and denominator,

$$\chi_{\hbar,ij}(\mathbf{q}) = \frac{n_{ij}(q_x, q_y)}{d(q_x, q_y)}, \quad (62)$$

where the latter is given by

$$\begin{aligned} d(q_x, q_y) = & \left( \frac{q_x^2 + q_y^2}{2m} \right)^2 - (2\delta_p - 4V|\psi_0|^2) \frac{q_x^2 + q_y^2}{2m} \\ & - \frac{k_p^2 q_x^2}{m^2} + \frac{2i\kappa k_p q_x}{m} + 3V^2 |\psi_0|^4 \\ & - 4\delta_p V |\psi_0|^2 + \delta_p^2 + \kappa^2. \end{aligned} \quad (63)$$

The last line above is zero in the regime we are investigating, as that is the condition for a gapless spectrum. Consequently, in the long-range limit,  $d$  will go to zero and the response function will exhibit singular behavior. To discover whether this may be superfluid behavior, we must look at the limiting behavior of the numerator.

From Eq. (60), the numerator of the  $\chi_{\hbar,xx}$  component is given by

$$\begin{aligned} n_{xx}(q_x, q_y) = & \frac{|\psi_0|^2}{2m^2} \left[ \frac{q_x^4}{2m} + \frac{q_x^2 q_y^2}{2m} \right. \\ & - \left. \left( \frac{2k_p^2}{m} + \delta_p - 3V|\psi_0|^2 \right) q_x^2 \right. \\ & \left. + \frac{2k_p^2}{m} q_y^2 + 4ik_p \kappa q_x - 4k_p^2 (\delta_p - V|\psi_0|^2) \right]. \end{aligned} \quad (64)$$

The limits of this expression are different depending on whether  $\mathbf{k}_p \neq 0$ , the anisotropic case, or whether  $\mathbf{k}_p = 0$ , the isotropic case. We will deal with each in turn.

#### A. Anisotropic case

In the anisotropic case, choosing  $\mathbf{k}_p$  in the  $x$  direction without loss of generality, we may study the response to an  $x$ -directed perturbation through  $n_{xx}$ . Taking the limits of the above expressions in the correct order, one finds the following behavior for the longitudinal and transverse responses:

$$\lim_{\mathbf{q} \rightarrow 0} \chi_{\hbar,xx,L}(\mathbf{q}) = \frac{C_1}{|\mathbf{q}| \rightarrow 0}, \quad (65)$$

$$\lim_{\mathbf{q} \rightarrow 0} \chi_{\hbar,xx,T}(\mathbf{q}) = \frac{C_2}{(|\mathbf{q}| \rightarrow 0)^2}, \quad (66)$$

for some constants  $C_1$  and  $C_2$ . Performing the equivalent calculations, starting again from Eq. (60), for the off-diagonal components,  $\chi_{\hbar,xy}$  and  $\chi_{\hbar,yx}$ , we also encounter divergences, and it is tempting to ask whether any physical conclusions can be drawn from any of these cases. The  $\chi_{\hbar,yy}$  component of the response function, however, is equivalent to the isotropic  $\chi_{\hbar,xx}$  case (due to our choice of  $\mathbf{k}_p$ ), to which we now turn.

#### B. Isotropic case

Taking the correct limits in the isotropic case, it is found that

$$\lim_{\mathbf{q} \rightarrow 0} \chi_{\hbar,xx,L}(\mathbf{q}) = \frac{|\psi_0|^2 (\delta_p - 3V|\psi_0|^2)}{m(2\delta_p - 4V|\psi_0|^2)}, \quad (67)$$

$$\lim_{\mathbf{q} \rightarrow 0} \chi_{\hbar,xx,T}(\mathbf{q}) = 0, \quad (68)$$

and that  $\chi_{\hbar,xy} = \chi_{\hbar,yx} = 0$ . This would appear to strongly suggest superfluid behavior. It is not clear, however, whether this conclusion extends to  $O(\hbar^2)$ , and what the mechanism for this superfluidity would be in the absence of a global  $U(1)$  symmetry.

In the following sections of this paper we will answer these questions, starting with the anisotropic, finite  $\mathbf{k}_p$  case in Sec. IV, and continuing with the isotropic  $\mathbf{k}_p = 0$  case in Sec. V.

### IV. DIVERGING ANISOTROPIC RESPONSE

#### A. Catastrophe structure of the mean-field solutions

Before directly tackling the origin of the divergent response, it is helpful first to analyze further the structure of the system's mean field, since it is here that the answer will be shown to reside. Let us thus return to Eq. (16) for the homogeneous mean-field solutions

$$V^2 n^3 - 2\delta_p V n^2 + (\delta_p^2 + \kappa^2) n - F_p^2 = 0. \quad (69)$$

This equation may be rewritten as

$$\partial_n \left[ \frac{1}{4} V^2 n^4 - \frac{2}{3} \delta_p V n^3 + \frac{1}{2} (\delta_p^2 + \kappa^2) n^2 - F_p^2 n \right] = 0, \quad (70)$$

indicating that these mean-field solutions correspond to extrema of the effective potential

$$U_{\text{eff}}(n) = \frac{1}{4} V^2 n^4 - \frac{2}{3} \delta_p V n^3 + \frac{1}{2} (\delta_p^2 + \kappa^2) n^2 - F_p^2 n. \quad (71)$$

Moreover,

$$\text{Im } \omega^+(\mathbf{0}) = -\kappa + \text{Im } \sqrt{3V^2 n^2 - 4\delta_p V n + \delta_p^2}, \quad (72)$$

so a sufficient condition for dynamical instability  $\text{Im } \omega^+(\mathbf{0}) > 0$  may be written as

$$3V^2 n^2 - 4\delta_p V n + \delta_p^2 < -\kappa^2, \quad (73)$$

or

$$\partial_n^2 U_{\text{eff}} < 0. \quad (74)$$

We may reduce  $U_{\text{eff}}$  to a standard form by eliminating the cubic coefficient via a linear variable change  $n = m + \frac{2\delta_p}{3V}$ , discarding the constant term (which does not contribute to any derivatives), and subsequently dividing through by the quartic coefficient, yielding

$$\begin{aligned} U'_{\text{eff}}(m) = & m^4 + \frac{2(3\kappa^2 - \delta_p^2)}{3V^2} m^2 + \left( \frac{8\delta_p(\delta_p^2 + 9\kappa^2)}{27V^3} - \frac{4F_p^2}{V^2} \right) m. \end{aligned} \quad (75)$$

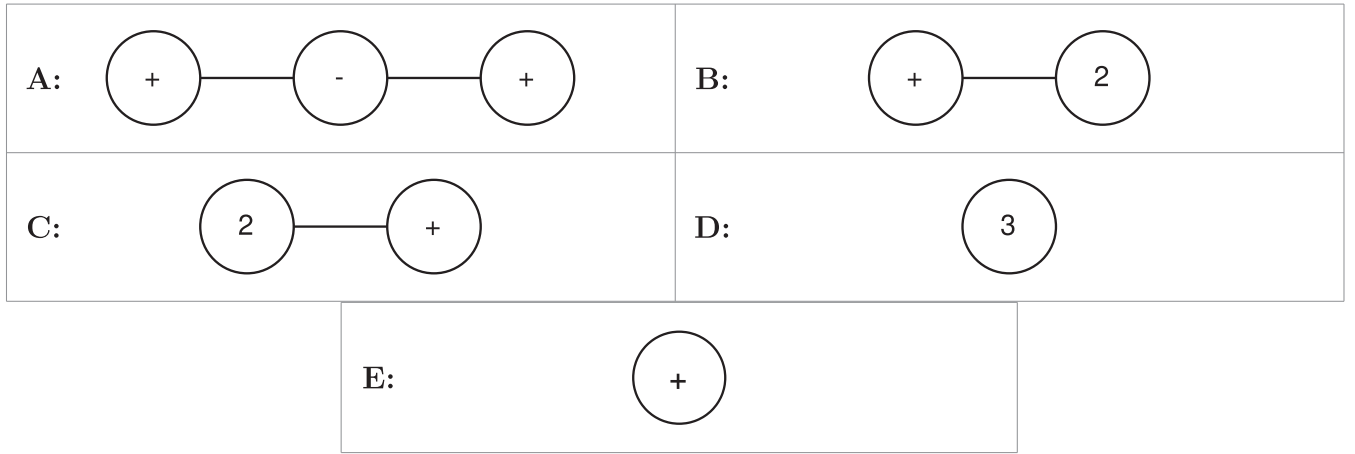


FIG. 5. Since it is globally expressible as the universal unfolding of a cusp catastrophe, there are five distinct topological configurations for the critical points of the effective potential  $U'_{\text{eff}}(m)$ . These are presented in the notation of Appendix C.

Introducing control parameters  $A(\delta_p) = \frac{2(3\kappa^2 - \delta_p^2)}{3V^2}$ ,  $B(\delta_p, F_p) = \frac{8\delta_p(\delta_p^2 + 9\kappa^2)}{27V^3} - \frac{4F_p^2}{V^2}$ , this is

$$U'_{\text{eff}}(m) = m^4 + A(\delta_p)m^2 + B(\delta_p, F_p)m. \quad (76)$$

The reader familiar with catastrophe theory will recognize this as the universal unfolding of a cusp catastrophe. Catastrophe theory is a branch of bifurcation theory, studying how small changes in an effective potential can yield large changes in the structure of that potential's stationary points. This has clear applications to classical statistical mechanics, where a system's equilibrium state is typically determined by minima of a thermodynamic potential, and extends to mean-field theory when the equations of motion can be reduced to stationarity equations for an effective potential as above. A short mathematical introduction to catastrophe theory is given in Appendix C.

That the potential corresponds to this unfolding globally rather than in a local neighborhood of a critical point simplifies the analysis. Every possible topological configuration of extrema is given in Fig. 5, of which there are seen to be five, and for simplicity we classify points as stable or unstable based on the partial criterion of Eq. (73).

Non-Morse critical points are points with a vanishing second derivative, or  $\partial_m^2 U'_{\text{eff}}(m) = 0$ . Since such points are structurally unstable relative to the control parameters  $A$  and  $B$ , and thus relative to  $\delta_p$  and  $F_p$ , we see that such points correspond to phase transitions [60]. Here these are the coalesced critical points corresponding to configurations B, C, D in Fig. 5. Those of double multiplicity, B and C, locally correspond to fold bifurcations; an infinitesimal perturbation of the control parameters may split such a point into a stable-unstable pair (case A) or eliminate it entirely (case E). Such an elimination results in a discontinuous collapse to the remaining stable critical point, meaning these are zero-order phase transition points. The point of triple multiplicity D, when it is non-Morse (if it is Morse, then we are not in the bistable regime), is just the catastrophe germ for the cusp catastrophe, and thus corresponds to a continuous phase transition. A general infinitesimal perturbation of the control parameters will

continuously split it into two stable and one unstable critical point, which is the universal unfolding A.

In the rest of the paper, it will be seen that it is the presence of these structurally unstable non-Morse critical points and their accompanying phase transitions that is the cause of the divergences appearing in the anisotropic current-current linear response. We may note already that the condition for a diverging linear response, a gapless spectrum, corresponds to the inequality in Eqs. (72) and (73) becoming an equality. This is precisely the condition for a non-Morse critical point.

Finally, we may visualize this catastrophe structure by solving  $\partial_m U'_{\text{eff}}(m) = 0$  for  $m$  in terms of  $A$  and  $B$ , and plotting the resulting  $m_{\text{soln}}(A, B)$ . This is seen in Fig. 6, where the resulting surface is called the “critical manifold” and the line of non-Morse critical points is termed the “locus of bifurcations.” By our stability criterion, the section of the surface inside the locus of bifurcations always corresponds to unstable solutions, while the section outside is generally stable (some of these points are unstable since our criterion is only partial, but this will not be relevant).

## B. The geometric origin of the divergence

### 1. Nonlinearity at the locus of bifurcations

Having laid the groundwork by identifying the presence of catastrophes and a locus of bifurcations in our system, we may now see how this leads to a diverging anisotropic response.

Consider the static mean-field equations for the anisotropic problem. Recall from Sec. IID 2 that the current-current response we seek is a response to the physical field  $f_i(\mathbf{q})$ , so we add the term  $\sum_{\mathbf{k}} \mathbf{f}(\mathbf{k}) \cdot \mathbf{j}^d(-\mathbf{k})$  to the action. Moreover, in the absence of an unphysical field, solutions to Keldysh mean-field equations have the quantum fields equal to zero so we preemptively set them so. The resulting equations are

$$\begin{aligned} (\Delta_p - \epsilon(\mathbf{k}) + i\kappa)\psi(\mathbf{k}) - F_p\delta_{\mathbf{k},0} \\ - \frac{V}{2} \sum_{\mathbf{k}', \mathbf{q}} \bar{\psi}(\mathbf{k}' + \mathbf{q})\psi(\mathbf{k} + \mathbf{q})\psi(\mathbf{k}') \\ + \sum_{\mathbf{q}} \gamma_i(2\mathbf{k} - \mathbf{q})f_i(\mathbf{q})\psi(\mathbf{k} - \mathbf{q}) = 0 \end{aligned} \quad (77)$$

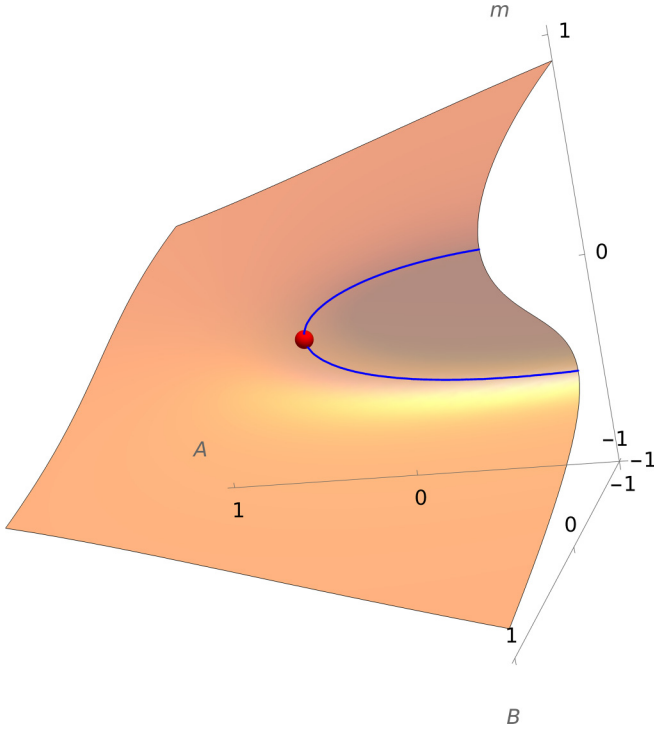


FIG. 6. Critical manifold of the solution  $m_{\text{soln}}(A, B)$  to  $\partial_m U'_{\text{eff}}(m) = 0$ . Solutions corresponding to non-Morse critical points form a line (blue) on this surface, called the locus of bifurcations; the name is due to infinitesimal perturbations in  $A$  and  $B$  at these points leading to a change in the number of solutions, i.e., to bifurcations. The critical point on this line corresponding to the cusp catastrophe germ is labeled by a red sphere.

and its complex conjugate. Splitting  $f_i(\mathbf{k})$  as  $f_i(\mathbf{k}) = f_i(\mathbf{0})\delta_{\mathbf{k},\mathbf{0}} + f_i(\mathbf{k})(1 - \delta_{\mathbf{k},\mathbf{0}})$  and temporarily setting the inhomogeneous components of the force to zero, the equations may be rewritten as

$$[\Delta_p + \gamma_i(2\mathbf{k})f_i(\mathbf{0}) - \epsilon(\mathbf{k}) + i\kappa]\psi(\mathbf{k}) - F_p\delta_{\mathbf{k},\mathbf{0}} - \frac{V}{2} \sum_{\mathbf{k}',\mathbf{q}} \bar{\psi}(\mathbf{k}' + \mathbf{q})\psi(\mathbf{k} + \mathbf{q})\psi(\mathbf{k}') = 0. \quad (78)$$

Finally consider homogeneous solutions:

$$[(\delta_p + \gamma_i(\mathbf{0})f_i(\mathbf{0})) + i\kappa]\psi_0 - F_p - V\psi_0|\psi_0|^2 = 0. \quad (79)$$

We see that the homogeneous component of the force couples into this equation in the same way as the detuning. We can thus absorb this into an effective  $\delta'_p = \delta_p + \gamma_i(\mathbf{0})f_i(\mathbf{0})$ .

Now, note that the mean-field value of the classical current is given by

$$j_{\text{mf},i}(\mathbf{q}) = \gamma_i(0)|\psi_0|^2\delta_{\mathbf{q},\mathbf{0}}, \quad (80)$$

so that the mean-field linear response to a homogeneous force can, with some caution, be viewed as

$$\chi_{\text{mf},ij}(0) = \gamma_i(0) \frac{\partial |\psi_0|^2}{\partial f_j(0)} = \gamma_i(0) \frac{\partial |\psi_0|^2}{\partial \delta'_p} \gamma_j(0), \quad (81)$$

and herein lies the connection. Looking at the control surface again, we see that along the locus of bifurcations  $\frac{\partial m}{\partial A}$  and  $\frac{\partial m}{\partial B}$  diverge. This is because, in a neighborhood of any point

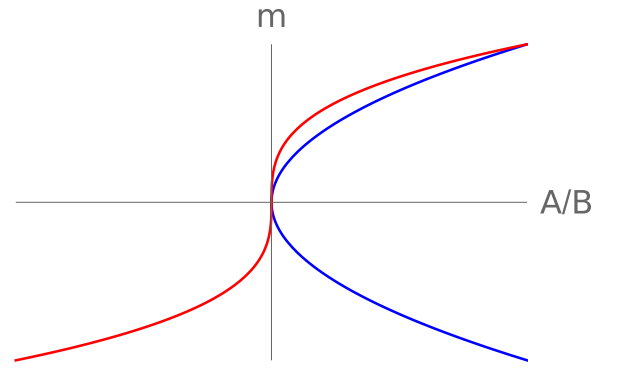


FIG. 7. A fixed- $A$  or - $B$  cross section of the critical manifold with a point of the locus of bifurcations at the origin will have one of the two general forms shown here. The blue line indicates the case of a twofold multiplicity point, while the red relates to the point of triple multiplicity. In both cases derivatives diverge at the origin, i.e., on the locus.

on the locus, a fixed- $A$  or - $B$  cross section will possess one of the two forms in Fig. 7. Such a divergence of the linear response to control parameters is typical of bifurcation points in catastrophe theory [61].

As a result, if we choose  $F_p$  and  $\delta_p$  such that  $m$  lies on the locus and  $m'$ , defined as  $m$  but with  $\delta'_p$  instead of  $\delta_p$ , is a stable solution, we find

$$\frac{\partial |\psi_0|^2}{\partial \delta'_p} = \frac{2}{3V} + \frac{\partial m'}{\partial A} \frac{\partial A}{\partial \delta'_p} + \frac{\partial m'}{\partial B} \frac{\partial B}{\partial \delta'_p}. \quad (82)$$

Thus, as  $\mathbf{f}(\mathbf{0}) \rightarrow 0$ , i.e.,  $\delta'_p \rightarrow \delta_p$ ,  $\frac{\partial |\psi_0|^2}{\partial \delta'_p} \rightarrow \infty$ . This shows that the divergence in the current-current response in this case is intimately tied to the presence of a bifurcation. Far from being unphysical, the divergence expresses the high degree of non-linearity present in the vicinity of a non-Morse critical point corresponding to a phase transition, and the mechanism just described is typical of the origin of divergent linear responses at phase transitions.

## 2. Directional dependence of the response

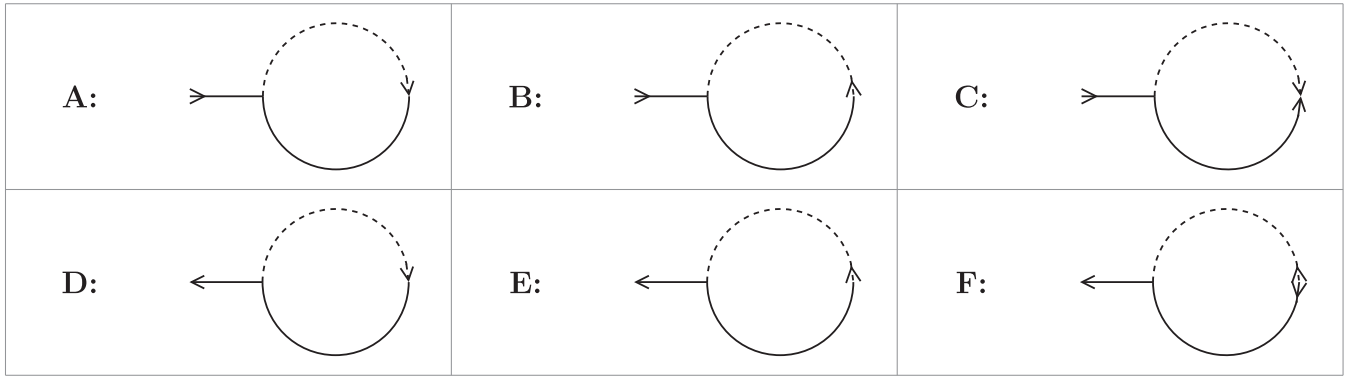
Equation (81),

$$\chi_{\text{hom-mf},ij} = \gamma_i(0) \frac{\partial |\psi_0|^2}{\partial f_j(0)},$$

is not entirely well founded. The limit  $\lim_{\mathbf{q} \rightarrow 0} \chi_{ij}(\mathbf{q})$  is sometimes directional (the definition of superfluid we are using relies on this fact), but the above expression admits no such possibility. In the case that this direction dependence is absent, however, we may show that the result agrees with a more rigorous treatment using the explicit form of the response tensor. In this case the response is just a measure of the change in occupation  $|\psi_0|^2$  of the macroscopically occupied pump state in response to an external static drive  $f_j(0)$ .

We begin by calculating  $\frac{\partial |\psi_0|^2}{\partial \delta_p}$ , or  $\frac{\partial n}{\partial \delta_p} = \dot{n}$ , by starting from the mean-field homogeneous equation:

$$V^2 n^3 - 2\delta_p V n^2 + (\delta_p^2 + \kappa^2)n - F_p^2 = 0. \quad (83)$$

FIG. 8.  $R/A$ -correlator tadpoles.

Differentiating,

$$3V^2n^2\dot{n} - 2Vn^2 - 4\delta_p Vn\dot{n} + 2\delta'_p n + (\delta_p^2 + \kappa^2)\dot{n} = 0, \quad (84)$$

and rearranging (provided the denominator is not 0),

$$\dot{n} = \frac{2Vn^2 - 2\delta_p n}{3V^2n^2 - 4\delta_p Vn + \delta_p^2 + \kappa^2}. \quad (85)$$

Our expression then yields

$$\begin{aligned} \chi_{\text{hom-mf},ij} &= -\frac{|\psi_0|^2(2\delta_p - 2V|\psi_0|^2)}{4m^2(3V^2|\psi_0|^4 - 4\delta_p V|\psi_0|^2 + \delta_p^2 + \kappa^2)} (\mathbf{k}_p)_i (\mathbf{k}_p)_j, \\ & \quad (86) \end{aligned}$$

which is identical to our  $O(\hbar)$  diagrammatic result in Eq. (61). We thus see that, where  $3V^2n^2 - 4\delta_p Vn + \delta_p^2 + \kappa^2 \neq 0$ , the limit is direction-independent and accurately captured by our formula. Moreover, we know that  $\partial_n^2 U_{\text{eff}}(n) = 3V^2n^2 - 4\delta_p Vn + \delta_p^2 + \kappa^2 = 0$  only on the locus of bifurcations, so  $\chi_{\text{hom-mf},ij} = \gamma_i(0) \frac{\partial |\psi_0|^2}{\partial f_j(0)}$  is valid as the locus is approached, and the divergence indeed arises from our earlier geometric argument.

## V. ISOTROPIC MEAN-FIELD SUPERFLUIDITY

We now turn to the isotropic case. Recalling the discussion of Sec. III B, we know that for  $\mathbf{k}_p = 0$  the  $O(\hbar)$  current-current

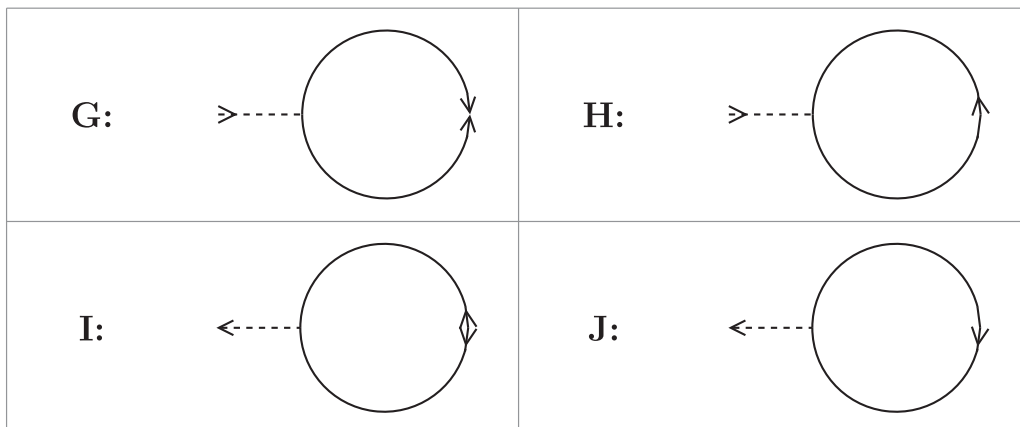
response is purely superfluid. This mean-field superfluidity has a curious origin as the interplay of two opposing processes; on the one hand, as the point of interest lies on the locus of bifurcations, the response for any nonzero pump momentum diverges for the geometric reasons as discussed in Sec. IV B. As  $k_p \rightarrow 0$ , however, the homogeneous component of the force couples increasingly weakly to the mean-field equations [its coupling being  $\gamma_i(\mathbf{0}) = \frac{k_p}{2m}$ ], and in the limit  $k_p = 0$  does not appear in them at all. This means that  $k_p \rightarrow 0$  leads to  $\chi_{\hbar}(\mathbf{0}) \rightarrow 0$  off of the locus and the interaction with the divergence at the locus yields a finite, nonzero superfluid response at it.

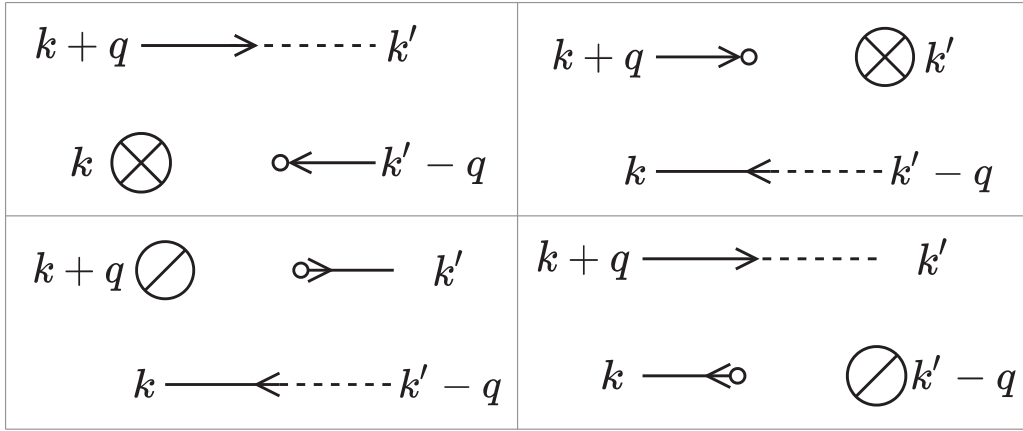
This elegant picture is unfortunately spoiled by higher-order terms in the perturbation expansion. We will now show that a divergence persists at  $O(\hbar^2)$ , and is related to the absence of  $U(1)$  symmetry in the problem.

### A. One-loop Keldysh tadpoles

One-loop tadpoles are truncated Feynman diagrams of the form  $\times \text{---} \bigcirc$ . There are six such tadpoles with  $R/A$  correlators as the loop, presented in Fig. 8, and four with a  $K$  correlator, presented in Fig. 9.

Crucially, the  $R/A$  loops are mutually canceling. To see this, consider the combination of terms coming from tadpoles (A) and (B) in Fig. 8 when attached to the same external line

FIG. 9.  $K$ -correlator tadpoles.


 FIG. 10.  $O(|\mathbf{q}|^0)$  diagrams, with the small circle denoting the tadpole attachment point.

on a diagram:

$$-G_X(0) \int dk (G_R^{11}(k) + G_A^{11}(k)) = 0. \quad (87)$$

Here  $G_X(0)$  is some correlator corresponding to the attachment, while the loops themselves are seen to cancel by the Keldysh relation  $\int d\omega [G_R(\omega) + G_A(\omega)] = 0$  (note that the  $\{11\}$  elements of the Keldysh matrices correspond to the true  $G_{R/A}$ ). Tadpoles (D) and (E) cancel in the same manner.

To see that tadpole (C) is zero, we write its attachment out explicitly:

$$\begin{aligned} & -G_X(0) \int dk G_R^{12}(k) \\ &= -G_X(0) \int dk \left( \int d\omega \frac{V \psi_0^2}{J(\omega, \mathbf{k}) J^*(-\omega, -\mathbf{k}) - V^2 |\psi_0|^4} \right). \end{aligned} \quad (88)$$

The denominator of the integrand is quadratic in  $\omega$ , and the pole lies in the lower half-plane (the denominator agrees with that of the true retarded Green's function). Thus, closing the contour in the upper half-plane, the integral is zero. The same reasoning then leads to the vanishing of tadpole (F).

The  $K$ -correlator tadpoles, however, do not cancel in this way. Moreover, when connected to an external line of a diagram, they introduce a term of the form  $G_{R/A}(0)$ . Such terms become singular in the limit of a gapless spectrum (since in that case the pole is precisely at  $\omega = 0$ ,  $\mathbf{k} = 0$ ) so that, for the perturbation expansion to remain finite, certain diagrams with external legs must vanish. We will now argue that this does not occur.

### B. Tadpole diagrams at $O(\hbar^2)$

Associating the connecting edge to the tadpole rather than to the main diagram, we see that a tadpole contributes  $\hbar$  to any diagram to which it is attached. This means that we are interested in cancellation of diagrams with a free leg that are  $O(\hbar)$  prior to the attachment of the tadpole.

To understand what kinds of diagrams may appear, we may apply some graph theory. Denote the number of 4-valent vertices by  $a$  and 3-valent vertices by  $b$ , the number of current fields participating in an edge (as opposed to assuming a mean-field value) by  $n$ , and the number of edges and vertices

by  $e$  and  $v$ , respectively. Then one finds (we subtract 1 because we do not count the edge connecting the tadpole)

$$\frac{4a + 3b - 1 - n}{2} + n = e, \quad (89)$$

$$a + b = v, \quad (90)$$

$$e - v = 1. \quad (91)$$

Here the last condition enforces that the diagram is  $O(\hbar)$ , since each vertex removes a factor of  $\hbar$  and each propagator or edge adds one. From here a little manipulation yields

$$2a + b = 3 - n, \quad (92)$$

which allows us to classify all possible diagrams.

We see that the possible values of  $n$  are  $n = 1, 2, 3$ . We may disregard  $n = 1$  because in this case three of the four current fields are set to mean-field values, meaning the remaining field is a quantum field. The attaching field of the  $K$ -tadpole is, however, also quantum and the quantum-quantum correlators are all zero, so that such diagrams vanish. For  $n = 2$ , the only possibility is  $b = 1$ , while for  $n = 3$  we must have  $a = b = 0$ . These are thus the only types of diagrams that we need consider.

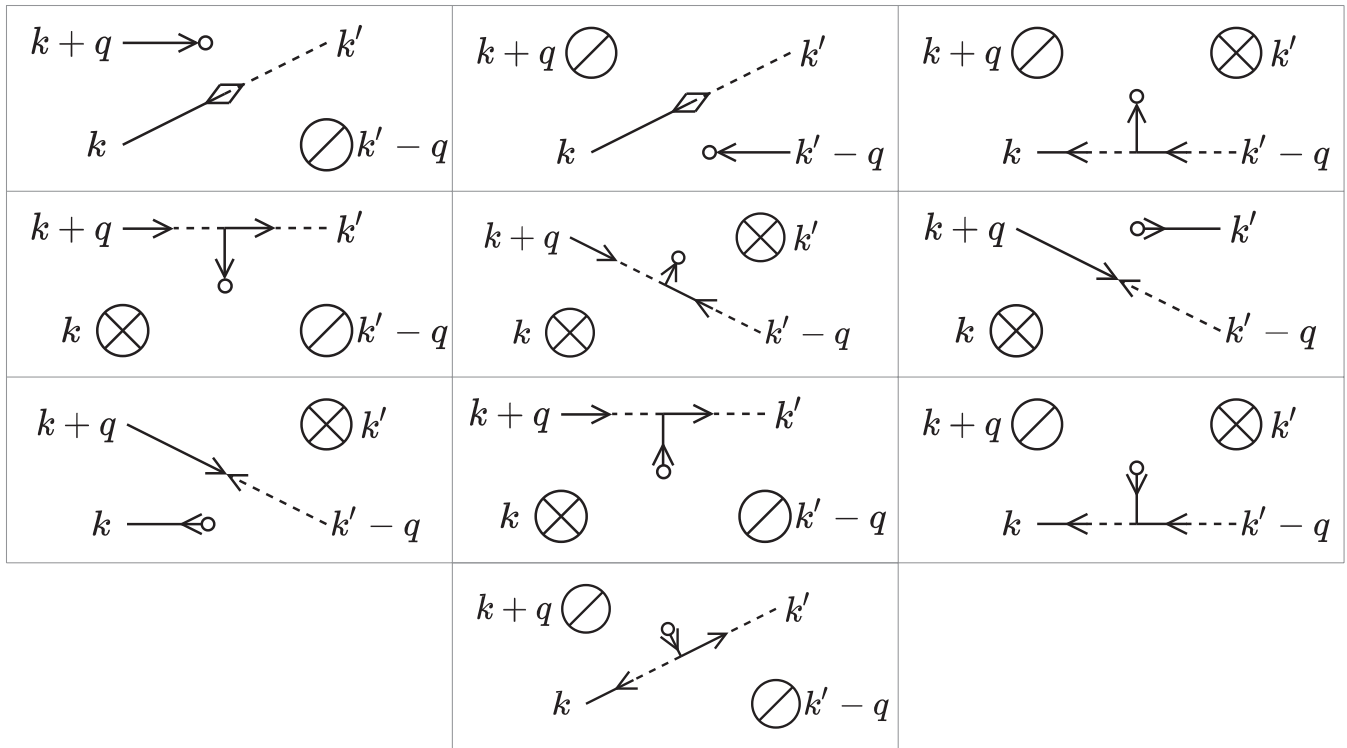
Unfortunately even after discarding those which trivially vanish, this still leaves a comparably large number: 32 diagrams. These diagrams, however, have different asymptotic dependencies on  $|\mathbf{q}| \rightarrow \infty$  (the momentum variable of the response function). Thus, to study whether these diagrams cancel, we may group them by this dependence; each group must cancel independently. Each diagram will possess two factors of  $\gamma(\pm\mathbf{q})$ . Furthermore,  $R/A$  correlators where the arrows match ( $G_{R/A}^{11}$  and  $G_{R/A}^{22}$ ) are  $O(|\mathbf{q}|^{-2})$ , while the others ( $G_{R/A}^{12}$  and  $G_{R/A}^{21}$ ) are  $O(|\mathbf{q}|^{-4})$ . We then have six diagrams of  $O(|\mathbf{q}|^{-6})$ , 12 diagrams of  $O(|\mathbf{q}|^{-4})$ , 10 diagrams of  $O(|\mathbf{q}|^{-2})$ , and four diagrams of  $O(|\mathbf{q}|^0)$ . These are given in Figs. 10–13.

We begin by considering the four  $O(|\mathbf{q}|^0)$  diagrams. The two with a  $\psi^c$  connecting field come out to

$$i\sqrt{2}[G_R^{11}(\mathbf{q}) + G_R^{22}(\mathbf{q})] \bar{\psi}_0 \gamma_i(\mathbf{q}) \gamma_j(\mathbf{q}), \quad (93)$$

while the other two yield

$$i\sqrt{2}[G_R^{11}(\mathbf{q}) + G_R^{22}(\mathbf{q})] \psi_0 \gamma_i(\mathbf{q}) \gamma_j(\mathbf{q}). \quad (94)$$


 FIG. 11.  $O(|\mathbf{q}|^{-2})$  diagrams, with the small circle denoting the tadpole attachment point.

Considering all possible  $K$ -tadpole attachments, we obtain the following expression for the sum of these diagrams:

$$\begin{aligned}
 & iV\sqrt{2}[G_R^{11}(\mathbf{q}) + G_R^{22}(\mathbf{q})]\gamma_i(\mathbf{q})\gamma_j(\mathbf{q})(\bar{\psi}_0[G_R^{11}(0)(\frac{1}{2}\bar{\psi}_0 \text{Tr}[G_K^{12}] + \psi_0 \text{Tr}[G_K^{11}]) + G_R^{12}(0)(\frac{1}{2}\psi_0 \text{Tr}[G_K^{21}] + \bar{\psi}_0 \text{Tr}[G_K^{22}])] \\
 & + \psi_0(G_R^{21}(0)(\frac{1}{2}\bar{\psi}_0 \text{Tr}[G_K^{12}] + \psi_0 \text{Tr}[G_K^{11}]) + G_R^{22}(0)(\frac{1}{2}\psi_0 \text{Tr}[G_K^{21}] + \bar{\psi}_0 \text{Tr}[G_K^{22}]))) . \quad (95)
 \end{aligned}$$

Denoting

$$a = \frac{1}{2}\bar{\psi}_0 \text{Tr}[G_K^{12}] + \psi_0 \text{Tr}[G_K^{11}], \quad (96)$$

$$b = \frac{1}{2}\psi_0 \text{Tr}[G_K^{21}] + \bar{\psi}_0 \text{Tr}[G_K^{22}], \quad (97)$$

the condition for this sum to be zero may be written as

$$\underbrace{\bar{\psi}_0 J^*(0)a + \bar{\psi}_0 V \psi_0^2 b}_{A} + \underbrace{\psi_0 V \bar{\psi}_0^2 a + \psi_0 J(0)b}_{-A} = 0. \quad (98)$$

Further, recalling that

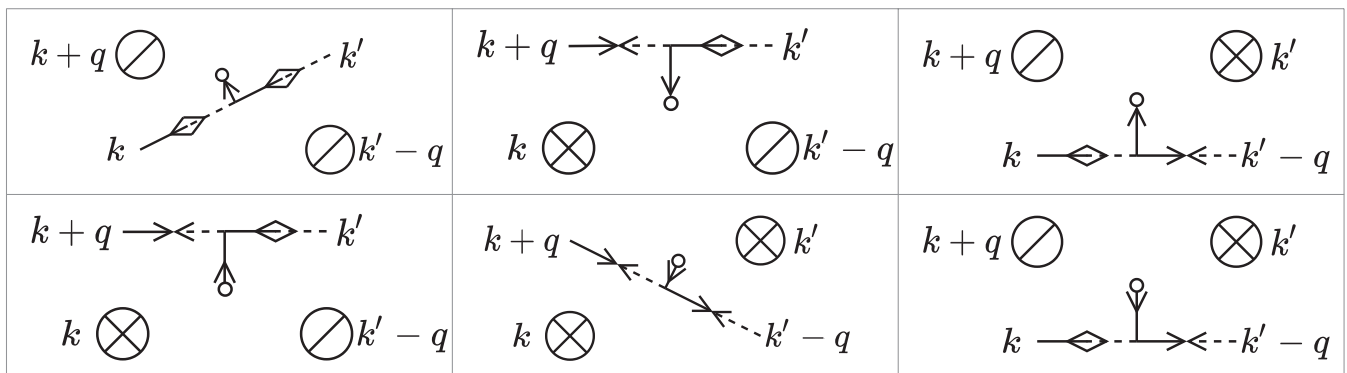
$$(G_R^{11}(k))^* = G_R^{22}(-k), \quad (99)$$

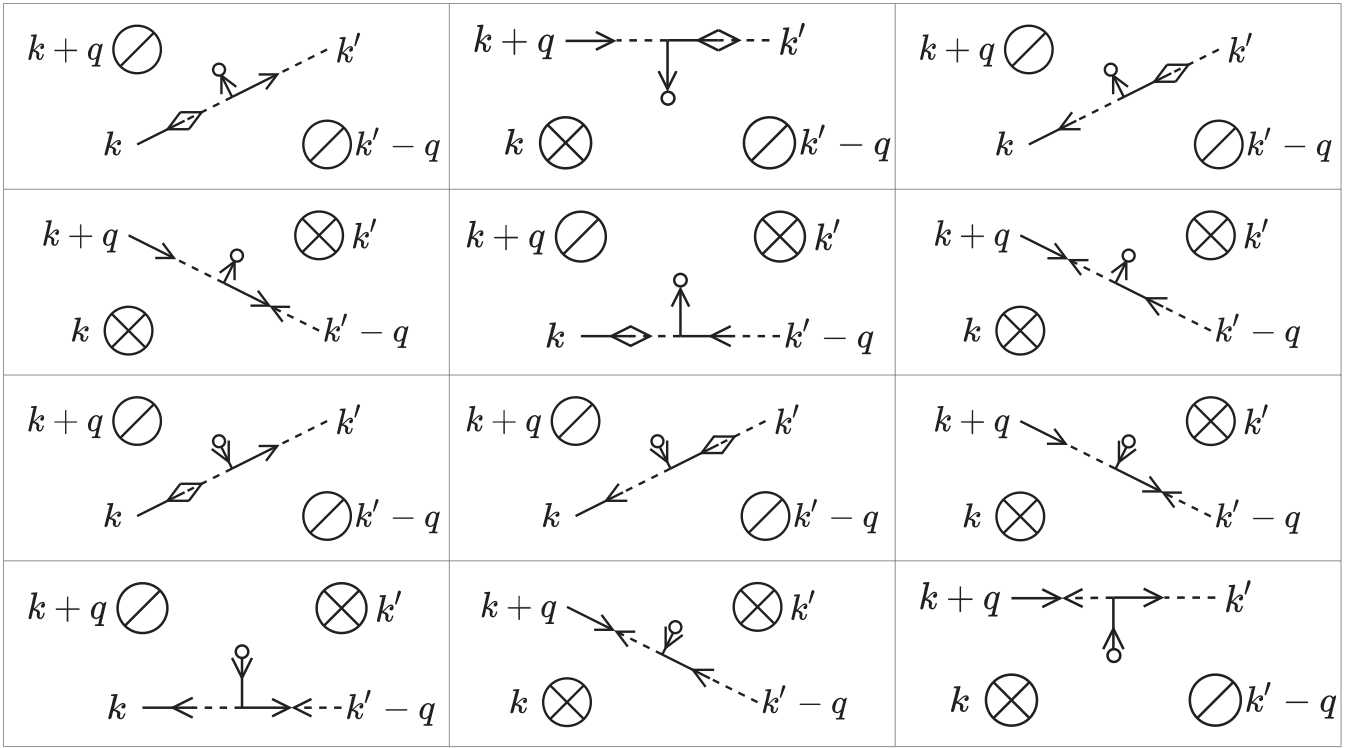
$$(G_R^{12}(k))^* = G_R^{21}(-k), \quad (100)$$

$$(G_K^{11}(k))^* = -G_K^{22}(-k), \quad (101)$$

$$(G_K^{12}(k))^* = -G_K^{21}(-k), \quad (102)$$

we have  $a^* = -b$ . This means that  $A = A^*$  so  $A$  is real.


 FIG. 12.  $O(|\mathbf{q}|^{-6})$  diagrams, with the small circle denoting the tadpole attachment point.


 FIG. 13.  $O(|q|^{-4})$  diagrams, with the small circle denoting the tadpole attachment point.

Setting  $A' = \frac{A}{|\psi_0|^2}$ , another real quantity, this equation may be rewritten as a matrix expression:

$$\begin{pmatrix} J^*(0) & -V\psi_0^2 \\ -V\bar{\psi}_0^2 & J(0) \end{pmatrix} \begin{pmatrix} a \\ a^* \end{pmatrix} = \begin{pmatrix} \psi_0 A' \\ \bar{\psi}_0 A' \end{pmatrix}. \quad (103)$$

Since this supposed cancellation is of interest only on the locus of bifurcations, we may specialize  $\psi_0$  to it. From Eq. (25) and the fact that the locus of bifurcations corresponds to a gapless complex spectrum, we find the condition ( $n = |\psi_0|^2$ )

$$3V^2 n^2 - 4\delta_p V n + \delta_p^2 + \kappa^2 = 0. \quad (104)$$

This may be combined with Eq. (14) to yield

$$\psi_0 = -\sqrt{n} \frac{Vn - \delta_p}{(Vn - \delta_p)^2 + \kappa^2} - i\sqrt{n} \frac{\kappa}{(Vn - \delta_p)^2 + \kappa^2}, \quad (105)$$

$$V\psi_0^2 = Vn \frac{(Vn - \delta_p)^2 - \kappa^2}{(Vn - \delta_p)^2 + \kappa^2} + iVn \frac{2\kappa(Vn - \delta_p)}{(Vn - \delta_p)^2 + \kappa^2}, \quad (106)$$

$$V\psi_0^2 = -\underbrace{\frac{2Vn(Vn - \delta_p)}{(Vn - \delta_p)^2 + \kappa^2}}_{=-1} J^*(0) = J^*(0). \quad (107)$$

From the last equation above we see that the matrix is degenerate, and the existence of a solution to (103) is not certain. To check this, we may decomplexify the matrix equation

via

$$\begin{pmatrix} M_{11}^r + iM_{11}^i & M_{12}^r + iM_{12}^i \\ M_{21}^r + iM_{21}^i & M_{22}^r + iM_{22}^i \end{pmatrix} \begin{pmatrix} x + iy \\ l + im \end{pmatrix} = \begin{pmatrix} v + iw \\ p + iq \end{pmatrix}$$

$\Downarrow$

$$\begin{pmatrix} M_{11}^r & -M_{11}^i & M_{12}^r & -M_{12}^i \\ M_{11}^i & M_{11}^r & M_{12}^i & M_{12}^r \\ M_{21}^r & -M_{21}^i & M_{22}^r & -M_{22}^i \\ M_{21}^i & M_{21}^r & M_{22}^i & M_{22}^r \end{pmatrix} \begin{pmatrix} x \\ y \\ l \\ m \end{pmatrix} = \begin{pmatrix} v \\ w \\ p \\ q \end{pmatrix}.$$

Applying this to (103) yields

$$2 \begin{pmatrix} \text{Im } J(0) \\ \text{Re } J(0) \\ \text{Im } J(0) \\ -\text{Re } J(0) \end{pmatrix} \text{Im } a = \begin{pmatrix} \text{Re } \psi_0 \\ \text{Im } \psi_0 \\ \text{Re } \psi_0 \\ -\text{Im } \psi_0 \end{pmatrix} A'. \quad (108)$$

Using (107), we must have

$$A' = 2 \frac{\text{Im } J(0)}{\text{Re } \psi_0} \text{Im } a = 4V\sqrt{n}\kappa \text{Im } a, \quad (109)$$

$$A' = 2 \frac{\text{Re } J(0)}{\text{Im } \psi_0} \text{Im } a = 2V\sqrt{n} \left( \kappa - \frac{(Vn - \delta_p)^2}{\kappa} \right) \text{Im } a. \quad (110)$$

Since  $\kappa > 0$ ,  $4\kappa \neq 2\left(\kappa - \frac{(Vn - \delta_p)^2}{\kappa}\right)$  so we must have  $\text{Im } a = A' = 0$ . Since  $\text{Im } a = 0$  implies  $A' = 0$ , we need consider only this condition:

$$\text{Im} \left( \frac{1}{2} \bar{\psi}_0 \text{Tr} [G_K^{12}] + \psi_0 \text{Tr} [G_K^{11}] \right) = 0. \quad (111)$$

Defining

$$D(k) = |J(k)J^*(-k) - V^2|\psi_0|^4|^2, \quad (112)$$

this is

$$\begin{aligned} -2i\kappa \int dk \frac{1}{D(k)} & \left( [|J(-k)|^2 + V^2|\psi_0|^4 - \epsilon(\mathbf{k})V|\psi_0|^2] \psi_0 \right. \\ & \left. + [V^2|\psi_0|^2] \psi_0^3 \right) \in \mathbb{R}. \end{aligned} \quad (113)$$

To proceed, it is helpful to calculate  $\int d\omega \frac{1}{D(\omega, \mathbf{k})}$  and  $\int d\omega \frac{\omega^2}{D(\omega, \mathbf{k})}$  (the denominator here is even in  $\omega$  so any term of

the form  $\int d\omega \frac{\omega}{D(\omega, \mathbf{k})}$  is zero). This may be accomplished by casting  $D(k)$  in residue form via the equation for the spectrum (25):

$$D(\omega, \mathbf{k}) = (\omega - \omega_{\mathbf{k}}^-)(\omega - \omega_{\mathbf{k}}^+)[\omega - (\omega_{\mathbf{k}}^-)^*][\omega - (\omega_{\mathbf{k}}^+)^*]. \quad (114)$$

At large  $\omega$  this is  $O(\omega^{-4})$ , so we may close the contour of integration in the upper half-plane (we assume for the moment that the complex spectrum is stable and gapped), yielding

$$\int d\omega \frac{1}{D(k)} = \frac{2\pi i}{[(\omega_{\mathbf{k}}^+)^* - \omega_{\mathbf{k}}^-][(\omega_{\mathbf{k}}^+)^* - \omega_{\mathbf{k}}^+][(\omega_{\mathbf{k}}^+)^* - (\omega_{\mathbf{k}}^-)^*]} + \frac{2\pi i}{[(\omega_{\mathbf{k}}^-)^* - \omega_{\mathbf{k}}^-][(\omega_{\mathbf{k}}^-)^* - \omega_{\mathbf{k}}^+][(\omega_{\mathbf{k}}^-)^* - (\omega_{\mathbf{k}}^+)^*]}, \quad (115)$$

$$\int d\omega \frac{\omega^2}{D(k)} = \frac{2\pi i((\omega_{\mathbf{k}}^+)^*)^2}{[(\omega_{\mathbf{k}}^+)^* - \omega_{\mathbf{k}}^-][(\omega_{\mathbf{k}}^+)^* - \omega_{\mathbf{k}}^+][(\omega_{\mathbf{k}}^+)^* - (\omega_{\mathbf{k}}^-)^*]} + \frac{2\pi i((\omega_{\mathbf{k}}^-)^*)^2}{[(\omega_{\mathbf{k}}^-)^* - \omega_{\mathbf{k}}^-][(\omega_{\mathbf{k}}^-)^* - \omega_{\mathbf{k}}^+][(\omega_{\mathbf{k}}^-)^* - (\omega_{\mathbf{k}}^+)^*]}. \quad (116)$$

Denoting

$$z = \sqrt{[\epsilon(\mathbf{k}) - \delta_p + 2V|\psi_0|^2]^2 - V^2|\psi_0|^4}, \quad (117)$$

$$\omega^\pm = -i\kappa \pm z, \quad (118)$$

we find

$$\int d\omega \frac{1}{D(k)} = \frac{8\pi\kappa}{z^4 - 2z^2[(z^*)^2 - 4\kappa^2] + [(z^*)^2 + 4\kappa^2]^2}, \quad (119)$$

$$\int d\omega \frac{\omega^2}{D(k)} = \frac{4\pi\kappa[z^2 + (z^*)^2 + 2\kappa^2]}{z^4 - 2z^2[(z^*)^2 - 4\kappa^2] + [(z^*)^2 + 4\kappa^2]^2}. \quad (120)$$

The above results were worked out on the assumption that the spectrum is stable and gapped. This may be viewed as a regularization of the gapless case, and we may now study the behavior of the above expressions for a gapless spectrum and  $\mathbf{k} \rightarrow 0$ . In this case, some algebra yields

$$\int d\omega \frac{1}{D(k)} \sim \frac{m\pi}{2(2V|\psi_0|^2 - \delta_p)\kappa} \frac{1}{|\mathbf{k}|^2 + \epsilon}, \quad (121)$$

$$\int d\omega \frac{\omega^2}{D(k)} \sim \frac{\pi}{2\kappa}. \quad (122)$$

Here  $\epsilon$  is a quantity that tends to zero as we go from a gapped to a gapless spectrum. The important consequence of this is that for a gapless spectrum, traces over the first of these quantities yield logarithmic divergences:

$$\begin{aligned} \int dk \frac{1}{D(k)} &= \int_0^\Lambda dk k \int d\omega \frac{1}{D(\omega, k)} \\ &\sim \frac{m\pi}{2(2V|\psi_0|^2 - \delta_p)\kappa} \int_0^{\epsilon'} dk \frac{k}{k^2 + \epsilon} \\ &+ \int_{\epsilon'}^\Lambda dk k \int d\omega \frac{1}{D(\omega, k)} \end{aligned}$$

$$\begin{aligned} &= \frac{m\pi}{4(2V|\psi_0|^2 - \delta_p)\kappa} \log\left(\frac{\epsilon'^2 + \epsilon}{\epsilon}\right) \\ &+ \int_{\epsilon'}^\Lambda dk k \int d\omega \frac{1}{D(\omega, k)}. \end{aligned} \quad (123)$$

Above  $\epsilon'$  is some energy scale small enough for our small  $|\mathbf{k}|$  approximation to be valid,  $\Lambda$  is the cutoff of the effective field theory, and we have used rotational invariance to write the momentum integral as a one-dimensional integral over  $|\mathbf{k}|$ . For a fixed  $\kappa$ ,  $\epsilon$  may be shown to be polynomial in  $\delta_p$ , so that this logarithmic divergence differs from the polynomial divergences of the zero momentum correlators.

Traces over  $\frac{\epsilon(\mathbf{k})}{D(k)}$  are also seen to be finite [compare (121), noting that  $\epsilon(\mathbf{k}) \sim |\mathbf{k}|^2$  and the  $d\mathbf{k}$  integral has a cutoff], so that the logarithmically divergent terms in (113) are seen to be

$$-2i\kappa V^2 |\psi_0|^2 (2|\psi_0|^2 \psi_0 + \psi_0^3) \int dk \frac{1}{D(k)}. \quad (124)$$

The gapped-spectrum regularization of  $\int dk \frac{1}{D(k)}$  is real, so that the only way for the above expression to be real [recall that (113) being real is the condition for tadpole cancellation] is for  $|\psi_0|^2 \psi_0 + \psi_0^3$  to be purely imaginary. From (105), this is possible only if  $Vn - \delta_p = \pm \frac{\kappa}{\sqrt{3}}$ . Solving this equation [also recall that  $Vn$  is given by (31) at the inversion points] yields a single solution of  $\delta_p = \sqrt{3}\kappa$  when the inversion points coincide.

For any other relative magnitudes of  $\delta_p$  and  $\kappa$ , the condition fails to hold and the tadpole diagrams fail to cancel (moreover, they also possess the additional logarithmic divergences found above). This means that generically, as one approaches a non-Morse critical point of the system, the current-current linear response is perturbatively divergent beyond  $O(\hbar)$ , nullifying the mean-field result indicative of superfluidity.

The fact that the cancellation occurs at  $\delta_p = \sqrt{3}\kappa$ , the point corresponding to the monostable to bistable continuous phase transition, may suggest that something interesting may be occurring here. To this end we consider the remaining

terms

$$-2i\kappa \int dk \frac{1}{D(k)} (\omega^2 + \epsilon(\mathbf{k})^2 + \epsilon(\mathbf{k})(3V|\psi_0|^2 - 2\delta))\psi_0. \quad (125)$$

The bracket is multiplying  $\epsilon(\mathbf{k})$  is zero for  $\delta = \sqrt{3}\kappa$  (since  $V|\psi_0|^2 = \frac{2}{3}\delta$  in this case), so we are left with

$$-2i\kappa\psi_0 \int dk \frac{1}{D(k)} (\omega^2 + \epsilon(\mathbf{k})^2). \quad (126)$$

This is an integral of a real non-negative quantity and thus clearly greater than zero (the integrand is zero only at  $\omega = |\mathbf{k}| = 0$ ). For  $\delta_p = \sqrt{3}\kappa$ ,  $\psi_0 \propto 1 - \sqrt{3}i$ , so that the above expression cannot be purely real. This means that, even if the logarithmic divergences cancel at  $\delta_p = \sqrt{3}\kappa$ , the algebraic tadpole divergences do not and so the response still diverges.

Before proceeding, we should comment on our use of a classical drive term  $F_p$  despite performing calculations to  $O(\hbar^2)$ . Because all expectation values we calculate are in terms of the polariton fields only, any connected diagram involving the drive fields would contain either at least two polariton-drive correlators or a drive tadpole. We know that there are no tadpoles at mean field in the current-current response, so the drive fields would contribute only at  $O(\hbar^2)$ , namely, to the fluctuation calculations above. At that order, the drive tadpoles would replace polariton tadpoles in any diagram in which they appeared. Since these tadpoles would have a significantly different form to the polariton tadpoles, they would fail to cancel the divergences in the latter that we demonstrate, and our analysis would remain unchanged. The presence of two polariton-drive correlators would also not affect the divergences, and thus our analysis above is insensitive to this classical field simplification.

### C. Perturbative results and RG at non-Morse critical points

The above perturbative result is sufficient to cast serious doubt on the mean-field assertions of superfluidity we were investigating. That the higher-order fluctuation corrections are divergent is an example of the Ginzburg criterion at a phase transition, and indicates that mean field and, by extension, perturbation theory are not to be trusted. Mathematically, this is because perturbative results can be highly misleading in the vicinity of non-Morse critical points. Conventional perturbation theory relies on the Morse Lemma to locally approximate the integrand as Gaussian: if the lemma does not apply, integrals over the non-Morse or catastrophe part of the integrand may yield divergences in the perturbative scheme.

For integrals with a finite or countable number of modes such as simple path integral problems in quantum mechanics, the appearance of elementary catastrophes in the action yields certain special functions (e.g., the Airy function above) in an exact evaluation of the propagator or partition function, when a perturbative evaluation would fail [62]. In those simple cases, however, the essential variables or field modes were discrete and the action is purely real. Problems with a continuum of modes are typically studied via the renormalization group (RG), in light of which we may now consider the above result. Since RG is a subject considerably too vast to introduce here in a self-contained manner, it is suggested that the reader interested in this section but unfamiliar with RG first consult [63], which uses the same terminology and notation as we do here.

Consider the continuous phase transition at  $\delta_p = \sqrt{3}\kappa$ , and the following part of the Keldysh action:

$$\int dt d^2\mathbf{x} (\bar{\psi}^q (i\partial_t + \nabla^2)\psi^c + 2i\kappa|\psi^q|^2). \quad (127)$$

With two fields we are free to fix the behavior of two couplings under the RG flow and may also choose the dynamical exponent via anisotropic scaling. Choosing to fix the couplings of  $\bar{\psi}^q \nabla^2 \psi^c$ ,  $|\psi^q|^2$ , and choosing the dynamical exponent to be  $z = 2$  yields the following naive scaling dimensions:

$$[\psi^c] = 0, \quad (128)$$

$$[\psi^q] = 2. \quad (129)$$

If we consider a field coupled to a quantum current, this will add terms to the action of the form

$$\int dt d^2\mathbf{x} f^a(\mathbf{x}, t) \bar{\psi}^q \nabla_a \psi^c, \quad (130)$$

with  $[\psi^q \nabla \psi^c] = 3$ . If we consider very long-wavelength fields  $f^a$ , such that they may be considered essentially constant,  $f^a$  will then correspond to a relevant coupling; the addition of this term to the action at criticality will drive the system to a different RG fixed point, likely altering its behavior in a nonanalytic way. For this reason we expect the long-wavelength linear response to such a coupling to be divergent at the phase transition (in classical statistical mechanics such linear responses are typically second derivatives of an effective energy with names like ‘‘heat capacity’’ and ‘‘compressibility,’’ explaining why these transitions are often ‘‘second order’’).

By the above argument, that the low-wavelength current-current response at this phase transition diverged in our perturbative calculation is unsurprising. That it diverged at all wavelengths, however, is of interest. To get a more physical sense of why this occurs, let us focus on the divergent subexpression of (95):

$$\begin{aligned} & \bar{\psi}_0 (G_R^{11}(0) (\frac{1}{2} \bar{\psi}_0 \text{Tr} [G_K^{12}] + \psi_0 \text{Tr} [G_K^{11}]) + G_R^{12}(0) (\frac{1}{2} \psi_0 \text{Tr} [G_K^{21}] + \bar{\psi}_0 \text{Tr} [G_K^{22}])) \\ & + \psi_0 (G_R^{21}(0) (\frac{1}{2} \bar{\psi}_0 \text{Tr} [G_K^{12}] + \psi_0 \text{Tr} [G_K^{11}]) + G_R^{22}(0) (\frac{1}{2} \psi_0 \text{Tr} [G_K^{21}] + \bar{\psi}_0 \text{Tr} [G_K^{22}])). \end{aligned} \quad (131)$$

A little inspection shows that this is actually the  $O(\hbar)$  correction to  $\langle \psi^c(0)\bar{\psi}^c(0) \rangle$ , generated by diagrams of the form (mean field  $\psi$ )  $\times$  tadpole, which tells us that  $\langle \psi^c(0)\bar{\psi}^c(0) \rangle$  also perturbatively diverges. This is a classic manifestation of the Ginzburg criterion, with the field fluctuations exceeding the mean-field value at the transition. Looking at Figs. 3 and 10–13, we see that to  $O(\hbar^2)$  every diagram of the current-current is proportional either  $|\psi_0|^2$  or to this  $O(\hbar)$  correction. Intuitively this makes sense: the current response is proportional to the amount of condensate “available” to respond. Thus, if  $\langle \psi^c(0)\bar{\psi}^c(0) \rangle$  is divergent at a phase transition in a perturbative scheme, so too ought to be the current-current response.

The physical perturbative argument and RG theory argument combined give compelling evidence for the incorrectness of the mean-field superfluid result, and the absence of superfluid at this point. While the RG argument is not directly applicable to the rest of the locus of bifurcations, these points are all dynamically unstable and correspond to first-order phase transitions: one would thus *a priori* expect the linear response at them to also be nonanalytic, and the perturbative calculation seems to support this.

#### D. Comparison with incoherent drive

It is instructive to contrast the above cancellation failure with the case of isotropic incoherently driven polaritons, for which [31] established the presence of superfluidity. The Keldysh action of this model may be written as

$$\begin{aligned} \mathcal{S}_{\text{inc}} = & \sum_k (\bar{\psi}_k^c \quad \bar{\psi}_k^q) \begin{pmatrix} 0 & \bar{g}^{-1}(k) \\ (\bar{g}^{-1})^*(k) & 2i\kappa \end{pmatrix} \begin{pmatrix} \psi_k^c \\ \psi_k^q \end{pmatrix} \\ & - \frac{V}{2} \sum_{k,k',q} (\bar{\psi}_{k-q}^c \bar{\psi}_{k'+q}^q [\psi_k^c \psi_{k'}^c + \psi_k^q \psi_{k'}^q] + \text{c.c.}), \end{aligned} \quad (132)$$

$$\bar{g}^{-1} = \omega + \mu - \epsilon(\mathbf{k}) - i\kappa + ip(\omega + \mu), \quad (133)$$

$$p(\omega) = \gamma - \eta\omega, \quad \mu = \frac{\gamma - \kappa}{\eta}. \quad (134)$$

Here the  $F_p$  pump term of the coherent model has been replaced by the incoherent  $ip(\omega + \mu)$  pump term, where  $\mu$  is a chemical potential calculated from the condition for the existence of a macroscopically occupied mean field:

$$\mu + ip(\mu) - i\kappa = V|\psi_0|^2 \Rightarrow p(\mu) = \kappa. \quad (135)$$

Due to the great similarity of this effective action to that for coherently driven polaritons (9), the diagrammatics are identical up to a redefinition of  $|\psi_0|^2$  and  $J(k)$ . For the incoherent model these are given by

$$\tilde{J}(k) = \omega + \mu - \epsilon(\mathbf{k}) + i\kappa - ip(\omega + \mu) - 2V|\tilde{\psi}_0|^2, \quad (136)$$

$$V|\tilde{\psi}_0|^2 = \mu. \quad (137)$$

The condition for tadpole cancellation (98) studied in the preceding section carries over to the incoherent model via the  $J \rightarrow \tilde{J}$ ,  $\psi_0 \rightarrow \tilde{\psi}_0$  replacement. Since  $\tilde{J}(0) = -V|\tilde{\psi}_0|^2$ , the condition is satisfied and the diagrams do not cause a divergence in the gapless regime of the incoherent model.

From our above discussion we see that this also means a zero  $O(\hbar)$  correction to  $\langle \psi^c(0)\bar{\psi}^c(0) \rangle$ . Thus there is a well-defined value for the condensate, the current-current response is thus finite, and superfluidity is present as expected.

## VI. CONCLUSION

Early work [49,50] argued, via an appeal to the Landau criterion for a complex-valued spectrum, that coherently pumped systems below the OPO threshold could display superfluid behavior in a wide range of pump regimes despite the breaking of  $U(1)$  symmetry by the drive. We have reviewed these arguments in the context of subsequent work [51], which focused on a more rigorous definition of superfluidity via a system’s current-current response tensor as opposed to the Landau criterion, and showed that the steady states identified by the Landau criterion were not superfluid but rather a kind of rigid state which does not respond to either longitudinal or transverse perturbations (as opposed to a superfluid, which should respond longitudinally but not transversely). The present paper’s main focus is in turn concentrated on a restricted pump regime, namely inversion points of the bistability curve, where the excitation spectrum is gapless and mean-field calculations of the response tensor suggest superfluidity can nevertheless be found.

In the general anisotropic pump regime, we found that such inversion points exhibit diverging current-current responses. While the physical significance of these divergences was initially unclear, we demonstrated that they arise from a cusp-catastrophe structure present in the mean-field values of the system’s fields. The inversion points of interest correspond to the cusp’s “locus of bifurcations,” a line of solutions where small variations in system parameters lead to drastic changes in behavior due to possible bifurcations of the mean-field solution. It is generically true that at such points the linear response of the variables undergoing the bifurcation, here the system fields, diverges and we show how to relate the divergence of the linear current-current response to this.

Beyond that, in the isotropic case, we found that the mean-field current-current response at an inversion point is indicative of superfluidity. We show, however, that higher-order perturbative corrections at these points are divergent. These divergences may be viewed through either the lens of renormalization, which shows them to be driven by the current being a relevant operator, or via perturbation theory. In the latter, they arise due to a failure of Keldysh tadpole diagrams to cancel in a consistent manner. This cancellation failure induces a divergence in the condensate magnitude, which then yields a divergence in the current-current response. These divergences indicate that the mean-field superfluid result is not reliable, as is to be expected since the inversion points in fact correspond to phase transitions.

While in both cases the divergences arise from the phase-transition nature of points along the locus of bifurcations, we see that there are two different mechanisms at play: a purely geometric, catastrophe-theoretic mechanism which manifests at the mean-field level in the anisotropic regime, and a fluctuational “Ginzburg criterion” one that appears in both the isotropic and anisotropic regimes.

We have thus shown that initially promising mean-field results indicating superfluidity in the system are invalid, and there remain no known superfluid regimes in coherently driven exciton-polaritons. Nevertheless, there are remaining possible avenues of research. First, we have throughout considered a Markovian photon reservoir for the system, having demonstrated that an experimentally natural thermal reservoir will exhibit this property. Nevertheless, a number of recent works have considered the possibility of non-Markovian reservoir engineering (see [64] and Refs. 50–56 therein) to achieve various desired many-body states. While this seems unlikely to overcome the absence of  $U(1)$  symmetry in the system, it may nevertheless be worth investigating. Such an investigation, however, would be significantly more complicated than that in our present paper, as the resulting Keldysh action would be nontime local.

Another possible direction would be nonhomogeneous systems. For example, [65] considered scattering against a defect outside a coherently pumped spot, and observed suppressed scattering in the small region around the pump spot where the fluid velocity was below the sound velocity of the sonic regime. Since the  $U(1)$  symmetry of the fluid outside the pump region was not directly broken by the pump, there may be a possibility of engineering nonhomogeneous systems with regions of the polariton fluid being coherently pumped and others exhibiting superfluidity. While this may prove not to be the case (interactions with fluid flowing out of the pump spot may somehow still break the  $U(1)$  symmetry of the fluid outside), it is a possible interesting avenue to explore.

### ACKNOWLEDGMENTS

We thank J. Keeling for stimulating discussions. I.T. and M.H.S. gratefully acknowledge financial support from QuantERA InterPol and EPSRC (Grants No. EP/N509577/1, EP/T517793/1, EP/V026496/1, EP/S019669/1).

## APPENDIX A: EFFECTIVE KELDYSH ACTION

### 1. Nonequilibrium field theory

Zero-temperature perturbative QFT is often concerned with calculating time-ordered expectations of operators in a ground state  $|\Omega\rangle$ :

$$\begin{aligned} & \langle \mathcal{T} O_1(t_1) \dots O_n(t_n) \rangle \\ &= \frac{\langle \Omega | U(\infty, t_n) O_n \dots U(t_2, t_1) O_1 U(t_1, -\infty) | \Omega \rangle}{\langle \Omega | U(\infty, -\infty) | \Omega \rangle}. \end{aligned} \quad (\text{A1})$$

For a Hamiltonian consisting of creation and annihilation operators, the operator  $\langle \Omega | U(\infty, -\infty) | \Omega \rangle$  may be converted to a coherent state path integral expression (up to a phase factor that cancels in the ratio above) of the form

$$\langle \Omega | U(\infty, -\infty) | \Omega \rangle \propto \int_{\psi(-\infty)=\psi_{\text{in}}}^{\psi(\infty)=\psi_{\text{out}}} \mathcal{D}[\psi, \bar{\psi}] e^{iS} = G(\psi_{\text{out}}, \psi_{\text{in}}), \quad (\text{A2})$$

$$S = \int dt d\mathbf{x} (\bar{\psi} i \partial_t \psi - H(\bar{\psi}, \psi)), \quad (\text{A3})$$

via Trotter decomposition [62], where the boundary conditions  $\psi_{\text{in}}, \psi_{\text{out}}$  depend on the initial and final states. The numerator in the above ratio may then be calculated (up to the same phase factor) by taking functional derivatives of this object with a modified action:

$$\begin{aligned} & \langle \Omega | U(\infty, t_n) O_n \dots U(t_2, t_1) O_1 U(t_1, -\infty) | \Omega \rangle \\ & \propto \frac{\delta}{\delta J_1(t_1)} \dots \frac{\delta}{\delta J_n(t_n)} G_J(\psi_{\text{out}}, \psi_{\text{in}}) \Big|_{J=0}, \end{aligned} \quad (\text{A4})$$

$$S_J = S + \sum_{i=1}^n J_i O_i(\bar{\psi}, \psi). \quad (\text{A5})$$

The nonequilibrium situation is remarkably similar, but with a density matrix  $\rho_{-\infty}$  instead of a pure initial state  $|i\rangle$ . Supposing that the system obeys dynamical semi-group evolution  $\rho_t = \mathcal{E}_{t-t'}[\rho_{t'}]$ , Trotter decomposition again allows a path integral representation for objects of the form

$$\text{Tr} (\mathcal{E}_{\infty-t_n} [O_n \dots \mathcal{E}_{t_2-t_1} [O_1 \mathcal{E}_{t_1+\infty} [\rho_{-\infty}]]]). \quad (\text{A6})$$

In the case of Lindbladian evolution, a recipe for this is provided in [63]. In our case, since we have access to the driven Hamiltonian

$$\begin{aligned} H &= \sum_{\mathbf{k}} (\omega_{\text{LP}}(\mathbf{k} + \mathbf{k}_p) - \omega_p) a_{\mathbf{k}}^\dagger a_{\mathbf{k}} \\ &+ \frac{V}{2} \sum_{\mathbf{k}, \mathbf{k}', \mathbf{q}} a_{\mathbf{k}-\mathbf{q}}^\dagger a_{\mathbf{k}+\mathbf{q}}^\dagger a_{\mathbf{k}} a_{\mathbf{k}'} + \sum_{\mathbf{k}} \omega_A(\mathbf{p} + \mathbf{k}_p) A_{\mathbf{p}}^\dagger A_{\mathbf{p}} \\ &+ \sum_{\mathbf{k}, \mathbf{p}} \zeta_{\mathbf{k}, \mathbf{p}} (e^{i\omega_p t} a_{\mathbf{k}}^\dagger A_{\mathbf{p}} + A_{\mathbf{p}}^\dagger a_{\mathbf{k}} e^{-i\omega_p t}) + F_p (a_0^\dagger + a_0), \end{aligned} \quad (\text{A7})$$

we may instead apply the Feynman-Vernon method [66]. To this end, we first consider the evolution of an unphysical density matrix  $\rho_0 = |\psi_a\rangle\langle\psi_b|$ . To calculate the trace at time  $T$ , we may use the closed-system propagator to evolve each side:

$$\text{Tr} \rho_T = \int d\psi_T d\bar{\psi}_T \langle \psi_T | U(T, 0) | \psi_a \rangle \langle \psi_b | U(T, 0)^\dagger | \psi_T \rangle. \quad (\text{A8})$$

We know from (A3) how to represent each of the appearing objects as a functional integral. We then arrive at [going from a  $(T, 0)$  to a  $(\infty, -\infty)$  time range]

$$\text{Tr} \rho_\infty = \int_{\psi^-(\infty)=\psi_b}^{\psi^+(\infty)=\psi_a} \mathcal{D}[\psi^+, \bar{\psi}^+, \psi^-, \bar{\psi}^-] e^{iS}, \quad (\text{A9})$$

$$\begin{aligned} S &= \int dt d\mathbf{x} (\bar{\psi}^+ i \partial_t \psi^+ - H(\bar{\psi}^+, \psi^+) \\ &- \bar{\psi}^- i \partial_t \psi^- + H(\bar{\psi}^-, \psi^-)), \end{aligned} \quad (\text{A10})$$

with  $\psi^+$  coming from the path integral for  $\langle \psi_T | U(T, 0) | \psi_a \rangle$  and  $\psi^-$  from the path integral for  $\langle \psi_b | U(T, 0)^\dagger | \psi_T \rangle$ .

This construction is sometimes visualized as a time contour (the “Keldysh contour”) consisting of two parts. The first, the “forward contour,” runs from  $t = -\infty$  to  $t = \infty$  while the second, the “backward contour,” then runs back from  $t = \infty$  to  $t = -\infty$ . It is then stated that the  $\psi^+$  fields lie on the forward contour while the  $\psi^-$  fields lie on the backward contour.

The origin of this terminology may be seen by rearranging (A8) for a time range  $(\infty, -\infty)$  as

$$\begin{aligned} \text{Tr } \rho_\infty = & \int d\psi_\infty d\bar{\psi}_\infty \langle \psi_b | U(-\infty, \infty) | \psi_\infty \rangle \\ & \times \langle \psi_\infty | U(\infty, -\infty) | \psi_a \rangle \end{aligned} \quad (\text{A11})$$

and applying the resolution of identity for coherent states:

$$\text{Tr } \rho_\infty = \langle \psi_b | U(-\infty, \infty) U(\infty, -\infty) | \psi_a \rangle. \quad (\text{A12})$$

The expression on the right-hand side now looks like an evolution in time of the  $\psi_a$  state from  $t = -\infty$  to  $t = \infty$  along the forward contour followed by an evolution back in time from  $t = \infty$  to  $t = -\infty$  along the backward contour;  $\psi^+$  corresponds to the path integral for the first time evolution operator (the forward contour one) and  $\psi^-$  to the second operator (the backward contour one).

While the Keldysh contour picture is frequently referenced in the literature, it does not have a real physical meaning. As is clear from (A8), there is no backward evolution in time of a pure state but rather a forward evolution of a density matrix. The physical meaning of  $\psi^+$  is thus not of a field existing on a forward-evolving time contour but rather a field corresponding to the degrees of freedom of one of the Hilbert spaces (the left one) comprising the product Hilbert space in which the density matrix lies. Similarly,  $\psi^-$  corresponds to the degrees of freedom of the right Hilbert space. Nevertheless, the contour terminology is entrenched and we may occasionally use it.

Finally, we may discard some of the initial conditions and perform a change of variables. The former may be done because we shall be interested in an effective action for the evolution of a driven-dissipative subsystem of this system. Such systems typically possess a unique steady state [67] independent of the initial conditions, and this is the state in which we will be calculating correlators (since we have taken an infinite time interval). However, this must be done with care. The evolution will become driven-dissipative only after some bath is integrated out, and so initial conditions can be discarded only after this step; the initial conditions for the bath may contribute to a correct derivation of an effective action.

The latter is a variable change known as the Keldysh rotation and allows for the easy calculation of the system’s retarded, advanced, and kinetic Green’s functions. The transformation is unitary (hence the name “rotation”):

$$\begin{pmatrix} \psi^c \\ \psi^q \end{pmatrix} = \begin{pmatrix} \frac{1}{\sqrt{2}} & \frac{1}{\sqrt{2}} \\ \frac{1}{\sqrt{2}} & -\frac{1}{\sqrt{2}} \end{pmatrix} \begin{pmatrix} \psi^+ \\ \psi^- \end{pmatrix}, \quad (\text{A13})$$

and it may be shown that in these new variables [68]

$$iG_R(r) = \langle \psi^c(r) \bar{\psi}^q(0) \rangle, \quad (\text{A14})$$

$$iG_A(r) = \langle \bar{\psi}^c(r) \psi^q(0) \rangle, \quad (\text{A15})$$

$$iG_K(r) = \langle \psi^c(r) \bar{\psi}^c(0) \rangle, \quad (\text{A16})$$

$$0 = \langle \psi^q(r) \bar{\psi}^q(0) \rangle. \quad (\text{A17})$$

The fields  $\psi^c$  and  $\psi^q$  are known as the classical and quantum fields in Keldysh parlance. While their primary importance in this paper will be their utility for calculating the above Green’s functions, it bears to explain their naming and some of their other properties. This will hopefully also serve to show the connection between Keldysh theory and driven-dissipative Gross-Pitaevskii equations for those readers more familiar with the latter.

The typical structure of a bosonic Keldysh action is

$$\begin{aligned} \frac{1}{\hbar} \int dt d^d x [ & \bar{\psi}^q \text{CGPE}[\psi^c] + \psi^q \cdot \overline{\text{CGPE}[\psi^c]} \\ & + K[\psi^c] |\psi^q|^2 + O(|\psi^q|^3)], \end{aligned} \quad (\text{A18})$$

where we have temporarily reinserted  $\hbar$ , CGPE stands for “complex Gross-Pitaevskii equation,” and  $K[\psi^c]$  relates to the dissipation in the problem. If we rescale  $\psi^q \rightarrow \hbar \psi^q$  and  $K \rightarrow K/\hbar$  (the latter amounting to measuring the dissipation in units of energy [68]), we find the action to now be

$$\begin{aligned} \int dt d^d x [ & \bar{\psi}^q \cdot \text{CGPE}[\psi^c] + \psi^q \overline{\text{CGPE}[\psi^c]} \\ & + K[\psi^c] |\psi^q|^2 + O(\hbar^3 |\psi^q|^3)]. \end{aligned} \quad (\text{A19})$$

We thus see that in the  $\hbar \rightarrow 0$  limit, all terms in  $\psi^q$  of order higher than quadratic vanish. This is one of the reasons  $\psi^q$  is referred to as the quantum field—it is not present beyond quadratic order in the classical limit. Of the remaining terms, if  $K[\psi^c] = 0$ , the functional integral over  $\psi^q$  yields functional Dirac delta functions [via the functional version of the identity  $\int dx e^{ixy} = 2\pi \delta(y)$ ] strictly enforcing the CGPE for the classical field  $\psi^c$ . If the dissipative  $K$  term is not zero, it can be shown to convert the CGPE to a stochastic CGPE. This term thus introduces classical thermal or driven-dissipative effects into the problem [68].

This brings us to a second reason for the names of these fields. By the symmetry of the problem with respect to the forward and backward contours, it can be shown that  $\langle \psi^+ \rangle = \langle \psi^- \rangle$  and thus  $\langle \psi^c \rangle = \sqrt{2} \langle \psi^+ \rangle$ ,  $\langle \psi^q \rangle = 0$ . In this way, the classical field  $\psi^c$  is what captures the mean field of the problem (as we saw, it is the field that obeys the CGPE in the classical limit) while the quantum field is always zero in the mean field or classical limit.

## 2. Deriving the action

We are now ready to apply this method to (A7). Denoting the polariton and bath fields by  $\psi$  and  $\tau$  respectively, and grouping them via  $\Psi = (\psi^c, \psi^q)$ ,  $\tau = (\tau^c, \tau^q)$ , we find the

full action to be

$$\begin{aligned}
 S[\Psi, \tau] = \int dt \left[ \sum_{\mathbf{k}} \bar{\Psi}(t, \mathbf{k}) [i\partial_t + \omega_p - \omega_{LP}(\mathbf{k} + \mathbf{k}_p)] \sigma_1 \Psi(t, \mathbf{k}) - \sqrt{2} F_p [\bar{\psi}^q(t, \mathbf{0}) + \psi^q(t, \mathbf{0})] \right. \\
 + \sum_{\mathbf{p}} \bar{\tau}(t, \mathbf{p}) [i\partial_t - \omega_\tau(\mathbf{p})] \sigma_1 \tau(t, \mathbf{p}) - \sum_{\mathbf{k}, \mathbf{p}} \zeta_{\mathbf{k}, \mathbf{p}} (\bar{\tau}(t, \mathbf{p}) \sigma_1 \Psi(t, \mathbf{k}) e^{-i\omega_p t} + e^{i\omega_p t} \bar{\Psi}(t, \mathbf{k}) \sigma_1 \tau(t, \mathbf{p})) \\
 \left. - \sum_{\mathbf{k}, \mathbf{k}', \mathbf{q}} \frac{V}{2} (\Psi^T(t, \mathbf{k}) \Psi(t, \mathbf{k}') \bar{\psi}^c(t, \mathbf{k} - \mathbf{q}) \bar{\psi}^q(t, \mathbf{k}' + \mathbf{q}) + \text{c.c.}) \right], \quad (\text{A20})
 \end{aligned}$$

where  $\sigma_i$  denote the corresponding Pauli matrices. We may split off the part of this action containing the bath fields,

$$S_{\text{bath}}[\Psi, \tau] = \int dt \left[ \sum_{\mathbf{p}} \bar{\tau}(t, \mathbf{p}) [i\partial_t - \omega_\tau(\mathbf{p})] \sigma_1 \tau(t, \mathbf{p}) - \sum_{\mathbf{k}, \mathbf{p}} \zeta_{\mathbf{k}, \mathbf{p}} (\bar{\tau}(t, \mathbf{p}) \sigma_1 \Psi(t, \mathbf{k}) e^{-i\omega_p t} + e^{i\omega_p t} \bar{\Psi}(t, \mathbf{k}) \sigma_1 \tau(t, \mathbf{p})) \right], \quad (\text{A21})$$

and note that this term is quadratic in them. Performing the corresponding Gaussian integral yields

$$S_{\text{bath}}[\Psi] = - \int dt dt' \sum_{\mathbf{k}, \mathbf{k}', \mathbf{p}} \bar{\Psi}(t, \mathbf{k}) \sigma_1 \zeta_{\mathbf{k}, \mathbf{p}} \zeta_{\mathbf{k}', \mathbf{p}} e^{i\omega_p t} G_b(t - t') e^{-i\omega_p t'} \sigma_1 \Psi(t', \mathbf{k}'), \quad (\text{A22})$$

where  $G_b(t - t') = \delta(t - t') \{ [i\partial_t - \omega_\tau(\mathbf{p})] \sigma_1 \}^{-1}$ . At this stage, we must recall that the initial combined density matrix of the system and reservoir also makes a contribution to the functional integral; the combined system is nondissipative so there is no unique steady state that would allow us to discard the initial conditions.

The first assumption we will make is that the system begins in a tensor product state of the form

$$\rho_{\text{system}} \otimes \rho_{\text{bath}}.$$

This may be naturally achieved by supposing that we consider the combined system from the moment the system and bath first begin interacting. From here, we concentrate on  $\rho_{\text{bath}}$  since we will eventually be able to disregard  $\rho_{\text{system}}$ . This is because it will be  $\rho_{\text{system}}$  evolving in the final driven-dissipative problem, at which point there will be a unique steady state allowing us to disregard the initial density matrix.

The initial bath density matrix enters the problem by amending the term we have written as

$$\{ [i\partial_t - \omega_\tau(\mathbf{p})] \sigma_1 \}^{-1}.$$

With the density matrix accounted for and performing a Fourier transform,  $e^{i\omega_p t} G_b(t - t') e^{-i\omega_p t'}$  instead becomes [68]

$$\begin{aligned}
 \tilde{G}_b(\omega + \omega_p) \\
 = \begin{pmatrix} -2\pi i F(\omega + \omega_p) \delta(\omega + \omega_p - \omega_\tau) & \frac{1}{\omega + \omega_p - \omega_\tau + i\epsilon} \\ \frac{1}{\omega + \omega_p - \omega_\tau - i\epsilon} & 0 \end{pmatrix}, \quad (\text{A23})
 \end{aligned}$$

where  $F(\omega)$  is the ‘‘distribution function’’ corresponding to the bath density matrix. We now seek to show that, for reasonable choices of this initial distribution, the interaction of the polaritons with the reservoir will be Markovian and the resulting action will be time-local.

We can simplify further by assuming the coupling between the bath and the system is independent of the polariton momentum,  $\zeta_{\mathbf{k}, \mathbf{p}} \zeta_{\mathbf{k}', \mathbf{p}} = \zeta_{\mathbf{p}}^2$ , and by suggesting that, if the bath

frequencies  $\omega_\tau(\mathbf{p})$  form a dense spectrum and the coupling constants  $\zeta_{\mathbf{p}} = \zeta(\omega_\tau)$  are smooth functions of these, we can replace the sum over bath modes with the integral

$$\sum_{\mathbf{p}} \zeta_{\mathbf{p}}^2 \rightarrow \int d\omega_\tau \zeta(\omega_\tau)^2 N_\tau(\omega_\tau), \quad (\text{A24})$$

where  $N_\tau(\omega_\tau)$  is the bath density of states. The action then becomes

$$S_{\text{bath}}[\Psi] = - \int d\omega \sum_{\mathbf{k}} \bar{\Psi}(\omega, \mathbf{k}) \begin{pmatrix} 0 & d^A(\omega) \\ d^R(\omega) & d^K(\omega) \end{pmatrix} \Psi(\omega, \mathbf{k}), \quad (\text{A25})$$

with  $d^A(\omega)$ ,  $d^R(\omega)$ , and  $d^K(\omega)$  obtained via the Sokhotski-Plemelj theorem as

$$\begin{aligned}
 d^{R/A}(\omega) = \mathcal{P} \int d\omega_\tau \frac{\zeta(\omega_\tau)^2 N_\tau(\omega_\tau)}{\omega + \omega_p - \omega_\tau} \\
 \mp i\pi \zeta(\omega + \omega_p)^2 N_\tau(\omega + \omega_p), \quad (\text{A26})
 \end{aligned}$$

$$d^K(\omega) = -2\pi i F(\omega + \omega_p) \zeta(\omega + \omega_p)^2 N_\tau(\omega + \omega_p). \quad (\text{A27})$$

In order for the final action to be time-local or ‘‘Markovian,’’ the bath must appear to be frequency-independent to the system. To this end, recall that the system’s spectrum (that of the interacting lower polaritons) acts like the continuum analog of the natural frequency of an oscillator: the bath will interact with the system preferentially at these frequencies [68].

Due to our gauge transformation, the spectrum of the interacting polaritons is  $\omega_{LP}(\mathbf{k} + \mathbf{k}_p) - \omega_p$ . This has also, however, shifted  $F$ ,  $\zeta$ , and  $N_\tau$  in the  $d$  functions (A26) and (A27) via  $\omega \rightarrow \omega + \omega_p$ . Thus we may consider the variation of  $N(\omega_{LP}(\mathbf{k}))$ ,  $N(\omega_{LP}(\mathbf{k}))$ , and  $N(\omega_{LP}(\mathbf{k}))$  over the range of the lower polariton spectrum, assuming that  $\mathbf{k}_p$  is negligible relative to our momentum cutoff and that the interacting spectrum has roughly the same range as the bare spectrum (this is true in our weakly interacting case).

For exciton-polaritons, the bottom of the bare spectrum (and  $\omega_p$ , since we pump resonantly) is typically on the order of 1.5 eV [13] and the spectrum is bounded above by the exciton spectrum, the bottom of which is  $\sim 10$  meV higher. With exciton masses typically being between  $0.1m_e$  and  $1m_e$ , where  $m_e$  is the electron mass, we may crudely estimate the variation of the exciton spectrum up to the momentum cutoff of  $\frac{\hbar}{100\text{\AA}}$  as

$$\frac{1}{0.2m_e} \left( \frac{\hbar}{100\text{\AA}} \right)^2 \approx 0.15 \text{ eV}. \quad (\text{A28})$$

Together with the ghost branch of the polariton spectrum, this gives an approximate range of variation of  $1.5 \pm 0.15$  eV. We would thus like to argue that the variation of  $N$ ,  $\zeta$ , and  $F$  is negligible on it.

For a 3D photonic bath, the density of states  $N(\omega)$  will be quadratic in  $\omega$ , and a quick calculation shows that  $N_{\max} \approx 1.5N_{\min}$  on this range. Around the midpoint of these values,  $N(\omega_p)$ , the variation is on the order of 20%; for our purposes this sufficiently little variation to take this as constant.

We now turn to the frequency dependence in the bath's distribution function  $F$  and decay coupling  $\zeta$ . This is the point at which assumptions must be made about the initial density matrix. The most natural initial distribution for the bath would be thermal; it is a large reservoir which has equilibrated with its environment before coming into contact with the system. In this case the distribution function is  $F(\omega) = 2n_o(\omega) + 1$ , where  $n_o$  is the occupation number of the given energy level. If the bath is in thermal equilibrium at an energy scale significantly lower than the range of variation of the polariton spectrum, then at all relevant energies the occupation number

$n_o$  will be identically zero and the distribution function will be  $F(\omega) = 1$ . At the same time, we may expect the decay of the high energy polaritons to not occur preferentially into any of the equally empty photonic modes and thus set  $\zeta(\omega) = \zeta_{\text{const}}$ . In this case, setting  $\kappa = N(\omega_p)\zeta_{\text{const}}$  and  $F(\omega) = 1$ , we obtain from (A26) and (A27)

$$d^{R/A}(\omega) = \mp i\kappa, \quad (\text{A29})$$

$$d^K(\omega) = -2i\kappa. \quad (\text{A30})$$

We see that stipulating such an initial distribution yields a fully Markovian bath. It remains to check that the thermal distribution is indeed lower energy than the polaritons. With an average thermal photon energy of  $kT$ , at room temperature (300 K) this energy is 25 meV, which is significantly lower than the smallest energy in the cutoff polariton spectrum (roughly 1.35 eV). Thus the distribution has negligible occupation at the relevant energy levels as required.

While we have discussed a thermal distribution above, it being a natural experimental distribution, our arguments carry over to any distribution which may be expressed in terms of occupation numbers and which has occupancy only at energies significantly below those of the polaritons.

In this Markovian approximation, the final form of the action is

$$\begin{aligned} \mathcal{S}_{\text{eff}} = & \int dk \begin{pmatrix} \bar{\psi}_k^c & \bar{\psi}_k^q \end{pmatrix} \begin{pmatrix} 0 & g^{-1}(k) \\ (g^{-1})^*(k) & 2i\kappa \end{pmatrix} \begin{pmatrix} \psi_k^c \\ \psi_k^q \end{pmatrix} \\ & - \frac{V}{2} \int dk dk' dq \left( \bar{\psi}_{k-q}^c \bar{\psi}_{k'+q}^q [\psi_k^c \psi_{k'}^c \right. \\ & \left. + \psi_k^q \psi_{k'}^q] + \text{c.c.} \right) - \sqrt{2} F_p (\bar{\psi}_0^q + \psi_0^q), \end{aligned} \quad (\text{A31})$$

where  $g^{-1}(k) = \omega + \Delta_p - \omega_{LP}(\mathbf{k} + \mathbf{k}_p) - i\kappa$ .

## APPENDIX B: NAMBU DIAGRAMMATICS FOR THE KELDYSH ACTION

In the main body of the paper, a path integral over the action (9) is considered. This action may be written in terms of fluctuations  $(\delta\psi^c, \delta\psi^q)$  around the mean-field result  $(\psi^c, \psi^q) = (\sqrt{2}\psi_0, 0)$  worked out from (16). From here on we simply write  $(\psi^c, \psi^q)$  for these fluctuations. Such an expansion around the mean field will, however, contain quadratic fluctuation terms which do not fit the pattern of the quadratic term in the above action. These may be gathered in the following ‘‘Nambu’’ form [recall that  $J(k) = \omega + \Delta_p - \epsilon(\mathbf{k}) + i\kappa - 2V|\psi_0|^2$ ]:

$$\frac{1}{2} \int dk dk' \begin{pmatrix} \bar{\psi}^c(k') \\ \psi^c(-k') \\ \bar{\psi}^q(k') \\ \psi^q(-k') \end{pmatrix}^T \begin{pmatrix} 0 & 0 & J(k) & -V\psi_0^2 \\ 0 & 0 & -V\bar{\psi}_0^2 & J^*(-k) \\ J^*(k) & -V\psi_0^2 & 2i\kappa & 0 \\ -V\bar{\psi}_0^2 & J(-k) & 0 & 2i\kappa \end{pmatrix} \delta(k-k') \begin{pmatrix} \psi^c(k) \\ \bar{\psi}^c(-k) \\ \psi^q(k) \\ \bar{\psi}^q(-k) \end{pmatrix}, \quad (\text{B1})$$

but this introduces a certain redundancy of degrees of freedom. This redundancy arises from the fact that the complex variables in the Nambu vector  $\Psi(k) = (\psi^c(k), \bar{\psi}^c(-k), \psi^q(k), \bar{\psi}^q(-k))$  appear on both the left- and right-hand sides of the matrix as  $(k, k')$  vary. As a result, the Gaussian functional integral cannot be immediately performed via the standard form for  $z^\dagger M^{-1} z$  actions. Moreover, the associated measure  $\mathcal{D}\Psi(k)\mathcal{D}\bar{\Psi}(k')$  is redundant if a full range is taken for  $(k, k')$ .

The solution is to note that the action is invariant under the transformation  $(k, k') \rightarrow (-k', -k)$ . This transformation may be used to partition  $\mathbb{R}^8$  into two disjoint sets  $\Sigma$  and  $\Sigma'$  such that they transform into each other under it. There will be some ambiguity for elements of the form  $(k, -k)$  since they are invariant under it, but they represent a set of measure 0 and may thus be neglected. With this partition, the action may be rewritten as (note the elimination of the  $\frac{1}{2}$  factor to preserve the action due

to the halving of the integration volume)

$$\int_{\Sigma} dk dk' \begin{pmatrix} \bar{\psi}^c(k') \\ \psi^c(-k') \\ \bar{\psi}^q(k') \\ \psi^q(-k') \end{pmatrix}^T \begin{pmatrix} 0 & 0 & J(k) & -V\psi_0^2 \\ 0 & 0 & -V\bar{\psi}_0^2 & J^*(-k) \\ J^*(k) & -V\psi_0^2 & 2i\kappa & 0 \\ -V\bar{\psi}_0^2 & J(-k) & 0 & 2i\kappa \end{pmatrix} \delta(k-k') \begin{pmatrix} \psi^c(k) \\ \bar{\psi}^c(-k) \\ \psi^q(k) \\ \bar{\psi}^q(-k) \end{pmatrix}, \quad (\text{B2})$$

and the functional measure is also taken over  $\Sigma$ , eliminating its redundancy and reproducing the original measure.

It remains to observe that, were we to multiply this functional integral by another where we took  $\Sigma'$  as the integration range, we would again obtain a functional integral with action (B2) but the integration range unrestricted. Moreover, since in this new integral the field  $\psi(-k')$ ,  $(k, k') \in \Sigma$  in the left vector and  $\psi(-k')$ ,  $(-k', -k) \in \Sigma'$  in the right vector originate from two separate original integrals and are thus independent, the integral has no redundancy and is simply equal to the functional determinant of

$$\begin{pmatrix} 0 & 0 & J(k) & -V\psi_0^2 \\ 0 & 0 & -V\bar{\psi}_0^2 & J^*(-k) \\ J^*(k) & -V\psi_0^2 & 2i\kappa & 0 \\ -V\bar{\psi}_0^2 & J(-k) & 0 & 2i\kappa \end{pmatrix} \delta(k-k'). \quad (\text{B3})$$

Since the value of the original integral should not depend on whether  $\Sigma$  or  $\Sigma'$  was used, this means that it is equal to the square root of this functional determinant. We have seen in Appendix A that the path integral in this form corresponds to the trace of a time-evolved density matrix, so that this square root should be equal to 1.

From here we may add source terms of the form

$$\begin{pmatrix} J_1(k) \\ J_2(-k) \\ J_3(k) \\ J_4(-k) \end{pmatrix}^T \begin{pmatrix} \psi^c(k) \\ \bar{\psi}^c(-k) \\ \psi^q(k) \\ \bar{\psi}^q(-k) \end{pmatrix} + \begin{pmatrix} \bar{\psi}^c(k) \\ \psi^c(-k) \\ \bar{\psi}^q(k) \\ \psi^q(-k) \end{pmatrix}^T \begin{pmatrix} J_5(k) \\ J_6(-k) \\ J_7(k) \\ J_8(-k) \end{pmatrix} \quad (\text{B4})$$

to either the  $\Sigma$  or  $\Sigma'$  action, depending on which range of wave vectors we wish to study, and then perform the integral over the sum of the two actions. This will be a standard Gaussian integral with source terms, yielding

$$G[J_1, J_2, J_3, J_4, J_5, J_6, J_7, J_8] = \exp \left[ -i \int_{\tilde{\Sigma}} dk dk' \begin{pmatrix} J_1(k') \\ J_2(-k') \\ J_3(k') \\ J_4(-k') \end{pmatrix}^T \begin{pmatrix} 0 & 0 & J(k) & -V\psi_0^2 \\ 0 & 0 & -V\bar{\psi}_0^2 & J^*(-k) \\ J^*(k) & -V\psi_0^2 & 2i\kappa & 0 \\ -V\bar{\psi}_0^2 & J(-k) & 0 & 2i\kappa \end{pmatrix}^{-1} \begin{pmatrix} J_5(k) \\ J_6(-k) \\ J_7(k) \\ J_8(-k) \end{pmatrix} \right], \quad (\text{B5})$$

where we have denoted the integration range of the action to which we added the source terms by  $\tilde{\Sigma}$ . From here we observe that for  $(k, k') \in \tilde{\Sigma}$  (denoting the other integration range by  $\tilde{\Sigma}^c$ , the corresponding action by  $S_{\tilde{\Sigma}^c}$ , and the action with source terms and integration range  $\tilde{\Sigma}$  by  $S_{\tilde{\Sigma}, J}$ ),

$$\begin{aligned} & \langle (\psi_k^c)^a (\bar{\psi}_{-k}^c)^b (\psi_k^q)^c (\bar{\psi}_{-k}^q)^d (\bar{\psi}_k^c)^e (\psi_{-k}^c)^f (\bar{\psi}_k^q)^g (\psi_{-k}^q)^h \rangle \\ &= \frac{\delta^a}{\delta J_1(k)^a} \frac{\delta^b}{\delta J_2(-k)^b} \frac{\delta^c}{\delta J_3(k)^c} \frac{\delta^d}{\delta J_4(-k)^d} \frac{\delta^e}{\delta J_5(k)^e} \frac{\delta^f}{\delta J_6(-k)^f} \frac{\delta^g}{\delta J_7(k)^g} \frac{\delta^h}{\delta J_8(-k)^h} \int_{\tilde{\Sigma}} \mathcal{D}[\psi^c, \bar{\psi}^c, \psi^q, \bar{\psi}^q] \exp[iS_{\tilde{\Sigma}, J}] \\ &= \partial_J \left( \underbrace{\int_{\tilde{\Sigma}^c} \mathcal{D}[\psi^c, \bar{\psi}^c, \psi^q, \bar{\psi}^q] \exp[iS_{\tilde{\Sigma}^c}]}_1 \int_{\tilde{\Sigma}} \mathcal{D}[\psi^c, \bar{\psi}^c, \psi^q, \bar{\psi}^q] \exp[iS_{\tilde{\Sigma}, J}] \right) \\ &= \partial_J G[J_1, J_2, J_3, J_4, J_5, J_6, J_7, J_8]. \end{aligned} \quad (\text{B6})$$

This quadratic generating function structure for expectation values means that Wick's theorem will hold for diagrammatic calculations and, by selectively choosing  $\Sigma$ ,  $\Sigma'$ , and to which action to add the source terms, we may use the above formula to work out the expectation of the product of any pair of field modes. This yields the following correlators:

$$\left\langle \begin{pmatrix} \psi_k^c \\ \bar{\psi}_{-k}^c \end{pmatrix} \begin{pmatrix} \bar{\psi}_k^q & \psi_{-k}^q \end{pmatrix} \right\rangle = iG_R(k) = \frac{i}{J(k)J^*(-k) - V^2|\psi_0|^4} \begin{pmatrix} J^*(-k) & V\psi_0^2 \\ V\bar{\psi}_0^2 & J(k) \end{pmatrix}, \quad (\text{B7})$$

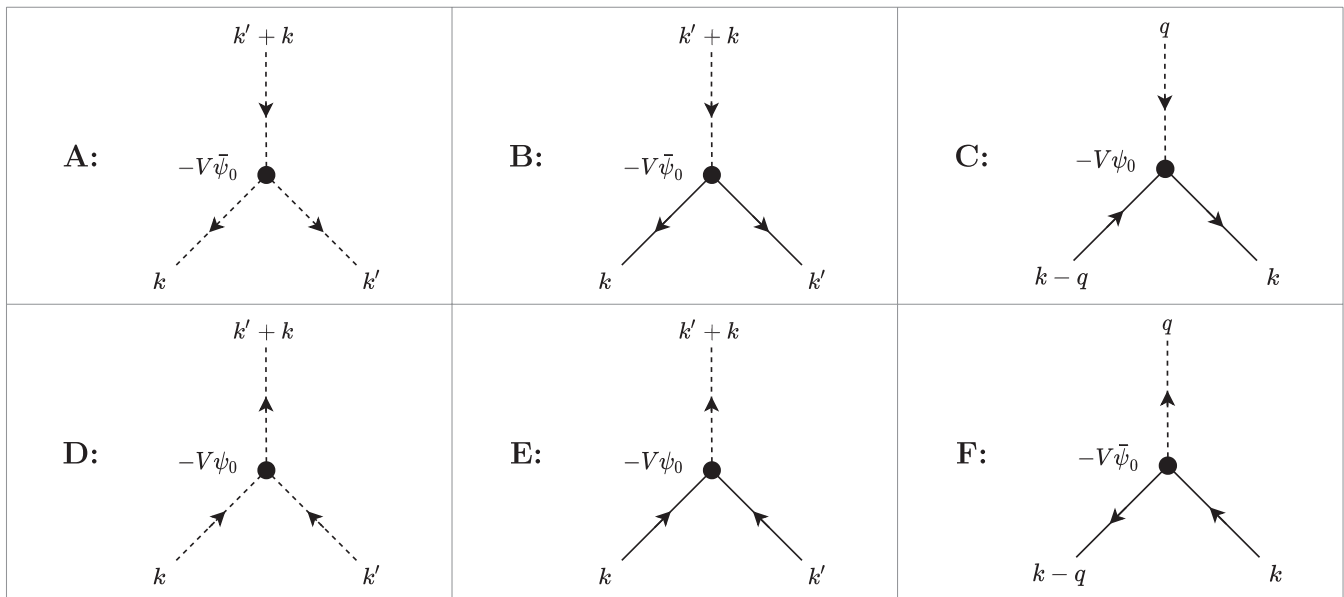


FIG. 14. Trivalent vertices of the quartic interaction.

$$\left\langle \left( \begin{array}{c} \psi_k^q \\ \bar{\psi}_{-k}^q \end{array} \right) (\bar{\psi}_k^c \quad \psi_{-k}^c) \right\rangle = iG_A(k) = \frac{i}{J(-k)J^*(k) - V^2|\psi_0|^4} \begin{pmatrix} J(-k) & V\psi_0^2 \\ V\bar{\psi}_0^2 & J^*(k) \end{pmatrix}, \quad (\text{B8})$$

$$\left\langle \left( \begin{array}{c} \psi_k^c \\ \bar{\psi}_{-k}^c \end{array} \right) (\bar{\psi}_k^q \quad \psi_{-k}^q) \right\rangle = iG_K(k) = \frac{2\kappa}{|J(k)J^*(-k) - V^2|\psi_0|^4|^2} \begin{pmatrix} J^*(-k)J(-k) + V^2|\psi_0|^4 & [J^*(-k) + J^*(k)]V\psi_0^2 \\ [J(-k) + J(k)]V\bar{\psi}_0^2 & J^*(k)J(k) + V^2|\psi_0|^4 \end{pmatrix}, \quad (\text{B9})$$

$$\left\langle \left( \begin{array}{c} \psi_k^q \\ \bar{\psi}_{-k}^q \end{array} \right) (\bar{\psi}_k^q \quad \psi_{-k}^q) \right\rangle = 0. \quad (\text{B10})$$

Since we expanded around the mean field, linear terms are removed from the action and quadratic ones have already been included in the matrix above, so it remains to consider the expansion of the quartic term

$$-\frac{V}{2} \int dk dk' dq (\bar{\psi}_{k-q}^c \bar{\psi}_{k'+q}^q [\psi_k^c \psi_{k'}^c + \psi_k^q \psi_{k'}^q] + \text{c.c.}) \quad (\text{B11})$$

into trivalent and tetravalent vertices to complete the standard diagrammatics. There are six topologically distinct trivalent vertices, and four tetravalent vertices, presented in Figs. 14 and 15 with their vertex factors. Standard rules for symmetry factors relating to exchange of vertices and edges then apply; symmetry multipliers have been included in the vertex factors, and it remains to divide a given diagram by its symmetry factor. Finally, since the expansion is taken around a nonzero value of  $\psi^c$ , diagrams may contain free  $\psi^c$  fields, corresponding to a factor of  $\psi_0$ , signified by circles with a line through them for  $\psi^c$  and a cross for  $\bar{\psi}^c$ .

### APPENDIX C: CATASTROPHE THEORY

Elementary catastrophe theory studies structurally unstable local behavior of functions. For systems controlled by the extremization of some effective potential, such local behavior of the extremum is frequently important [61]: for dynamical systems, the local behavior of potential minima affects their stability, while in the Landau mean-field theory of phases such behavior may lead to phase transitions. In the main body of the paper we find a situation where steady-state properties of a nonequilibrium may be obtained from the minima of a corresponding effective potential, and apply catastrophe theory to understand the resulting phenomena. We thus review catastrophe theory and its applications in this Appendix, following the exposition given in [61].

In its most elementary form, catastrophe theory is the extension of two fundamental results on the local behavior of functions, namely, a corollary of the Rectification Theorem for vector fields [69] and the Morse Lemma [60].

*Theorem 1 (Rectification Theorem (Corollary)).* Let  $f(x) = f(x_1, x_2, \dots, x_n)$  be a smooth function with nonzero gradient at  $x_0$ :

$$\nabla f|_{x_0} \neq 0. \quad (\text{C1})$$

Then there exists a neighborhood of  $x_0$  and a smooth change of coordinates,  $y = (y_1, y_2, \dots, y_n)$ ,  $y = y(x)$ , on this neighborhood so that

$$f(y) = y_1. \quad (\text{C2})$$

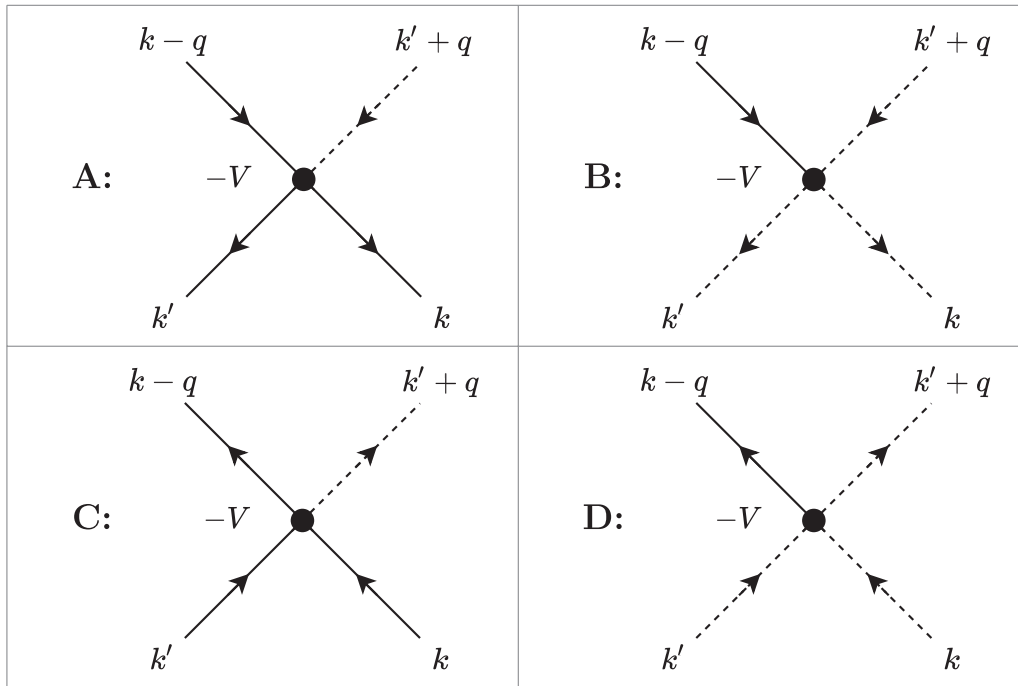


FIG. 15. Tetraivalent vertices of the quartic interaction.

*Theorem 2 (Morse Lemma).* Let  $f(x) = f(x_1, x_2, \dots, x_n)$  be a function with vanishing gradient and nonsingular Jacobian matrix at  $x_0$ :

$$\nabla f|_{x_0} = 0, \quad (\text{C3})$$

$$\det[\partial^2 f / \partial x_i \partial x_j]|_{x_0} \neq 0. \quad (\text{C4})$$

Then there exists a neighborhood of  $x_0$  and a smooth change of coordinates,  $y = (y_1, y_2, \dots, y_n)$ ,  $y = y(x)$ , on this neighborhood so that

$$f(y) = y_1^2 + y_2^2 + \dots + y_m^2 - y_{m+1}^2 - \dots - y_n^2, \quad (\text{C5})$$

where the number of positive and negative signs matches the Jacobian signature.

The first of these theorems describes the most common situation, away from a function's critical points, while the second describes the local behavior of nondegenerate, or "Morse," critical points. In particular, the Morse Lemma and related family of "Preparation Theorems" facilitate famous integral approximation methods such as Laplace's Method, the Method of Stationary Phase, and the Method of Steepest Descent, which are common in thermodynamic and QFT calculations.

A key feature of noncritical points and Morse critical points is known as "structural stability." Using the above theorems it may be shown that the addition of an infinitesimal perturbation to a function cannot change their nature; if a function  $f(x)$  possesses a noncritical or a Morse critical point at  $x_0$ , then for sufficiently small  $\epsilon$ , so will  $f(x) + \epsilon g(x)$  (the position of the critical point may shift infinitesimally but it will remain Morse).

Catastrophe theory, then, is concerned with situations where such structural stability is absent and so-called "catastrophes" may occur from infinitesimal perturbations. The bulk

of elementary catastrophe theory is contained in two further theorems, the Thom Splitting Lemma and Thom Classification Theorem.

*Theorem 3 (Thom Splitting Lemma).* Let  $f(x) = f(x_1, x_2, \dots, x_n)$  be a function with vanishing gradient and singular Jacobian matrix at  $x_0$ :

$$\nabla f|_{x_0} = 0, \quad (\text{C6})$$

$$\det[\partial^2 f / \partial x_i \partial x_j]|_{x_0} = 0. \quad (\text{C7})$$

If the Jacobian matrix possesses  $l$  vanishing eigenvalues, then there exists a neighborhood of  $x_0$  and a smooth change of coordinates,  $y = (y_1, y_2, \dots, y_n)$ ,  $y = y(x)$ , on this neighborhood so that the function splits as

$$f(y) = f_{NM}(y_1, \dots, y_l) + M(y_{l+1}, \dots, y_n), \quad (\text{C8})$$

$$M(y) = y_{l+1}^2 + y_{l+2}^2 + \dots + y_{l+m}^2 - y_{l+m+1}^2 - \dots - y_n^2, \quad (\text{C9})$$

$$f_{NM} \in O(y^3), \quad (\text{C10})$$

where  $M(y)$  is a structurally stable Morse component (the number of positive and negative signs again matches the signature of the Jacobian's nonzero eigenvalues) while  $f_{NM}$  is a structurally unstable non-Morse component.

The coordinates appearing in  $M$  are known as "inessential" since they do not participate in the dramatic structural instabilities associated with non-Morse behavior. Conversely, the coordinates appearing in  $f_{NM}$  are known as "essential." The Thom Classification Theorem seeks to classify the possible forms of the non-Morse component in the presence of external "control parameters," namely, variables  $c$  upon which a function  $f(x; c)$  depends but which are not coordinates [e.g., the mean and variance of a normal distribution  $\text{Norm}(x; \mu, \sigma)$ ].

*Theorem 4 (Thom Classification Theorem).* Let  $f_{NM}(x; c) = f(x_1, \dots, x_l; c_1, \dots, c_k)$  be a function of  $l$  coordinates and  $k$  control parameters, possessing a non-Morse critical point at  $x_0$ . Then there exists a neighborhood of  $x_0$  and a smooth change of coordinates,  $y = (y_1, y_2, \dots, y_n)$ ,  $y = y(x)$ , on this neighborhood so that the function takes the form of an elementary catastrophe function  $\text{Cat}$ :

$$f_{NM}(y; c) = \text{Cat}(y, c), \quad (\text{C11})$$

$$\text{Cat}(y, c) = \text{CG}(y) + \text{Pert}(y, c). \quad (\text{C12})$$

Every elementary catastrophe function consists of a catastrophe germ,  $\text{CG}$ , depending only on the coordinates, and a perturbation  $\text{Pert}$ , which is linearly dependent on the control parameters.

The possible canonical forms of catastrophe germs and perturbation terms are exhaustively catalogued for small numbers of coordinates and control parameters [61]. The addition of the most general perturbation to a given catastrophe germ is known as its universal unfolding. Structural instability comes from the dramatic effects of infinitesimal variations in the control parameters on the topology of the function's critical points. Such variations may locally create, merge, and annihilate critical points, in stark contrast to the stable regimes around noncritical and Morse critical points.

There exists a simple graphical notation for such topological configurations of critical points in the case of a function of a single coordinate. The idea is to draw a chain of circles corresponding to critical points, connected by lines and ordered from left to right per the ordering of the critical points along the real line. When the maximum possible number of critical points is present, maxima are denoted by a minus inside a circle and minima by a plus. In configurations where two or more critical points have just merged (creating a structurally unstable non-Morse critical point), the plus or minus is replaced by the number of merged critical points. If a critical point is annihilated in a configuration, that circle is removed. An example is given in Fig. 16. More sophisticated notation exists for the multivariate case [60] but will not be used in this paper.

We conclude this section by proving an important result that is used in the main paper. Suppose that a function  $f(x; c)$  possesses a critical point at  $x_c(c)$ , whose position depends smoothly on  $c$  and such that  $x_c(c_0) = x_0$ . We will now prove that the linear response  $dx_c/dc$  diverges if the critical point becomes non-Morse.

Expand  $f(x; c)$  in a Taylor series in both coordinates and control variables, taking  $\delta x$  and  $\delta c$  such that

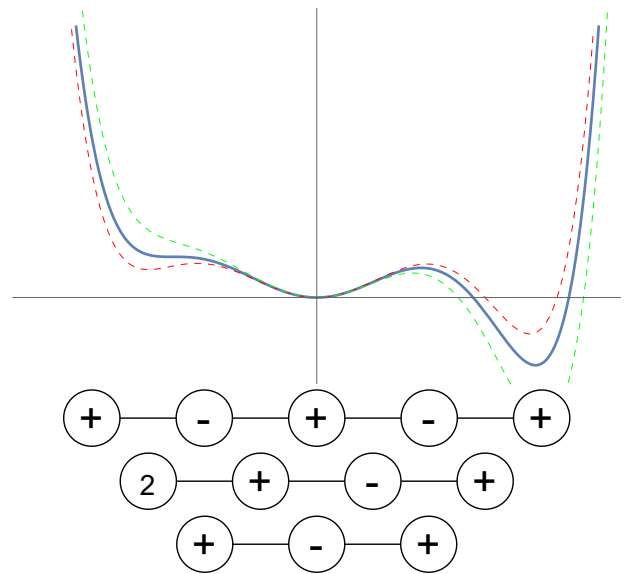


FIG. 16. Plot of a degree six polynomial for various values of its coefficients and the corresponding topological diagrams, showing how the diagrams change as the leftmost critical points merge and then annihilate. From top to bottom, the topological diagrams correspond to the red, blue, and green plots, respectively.

$$x_c(c_0 + \delta c) = x_0 + \delta x:$$

$$\begin{aligned} f(x_0 + \delta x; c_0 + \delta c) &= [f + \delta x_i \partial_i f + \delta c_a \partial_a f + \frac{1}{2} \delta x_i \delta x_j \partial_{ij} f + \delta x_i \delta c_a \partial_{ia} f \\ &\quad + \frac{1}{2} \delta c_a \delta c_b \partial_{ab} f + O(3)] \Big|_{x=x_0, c=c_0}. \end{aligned} \quad (\text{C13})$$

From this one obtains an expression for  $\frac{d}{dx} f(x_0 + \delta x, c_0 + \delta c)$ , which must be zero due to how we have chosen the increments:

$$\begin{aligned} \frac{d}{dx_i} f(x_0 + \delta x, c_0 + \delta c) &= [\partial_i f + \delta x_j \partial_{ij} f + \delta c_a \partial_{ia} f + O(3)] \Big|_{x=x_0, c=c_0}. \end{aligned} \quad (\text{C14})$$

$\partial_i f|_{x=x_0} = 0$  by the condition that  $x_0$  is a critical point, so we find

$$\delta x_j \partial_{ij} f + \delta c_a \partial_{ia} f = 0, \quad (\text{C15})$$

which yields

$$\frac{dx_{c,i}}{dc_a} = -[\partial^2 f]_{ij}^{-1} \partial_{ja} f. \quad (\text{C16})$$

If the critical point is non-Morse then  $\partial^2 f$  will be degenerate, and its inversion in the above formula will yield a divergent linear response.

- [1] P. Kapitza, Viscosity of liquid helium below the  $\lambda$ -point, *Nature (London)* **141**, 74 (1938).
- [2] J. F. Allen and A. Misener, Flow of liquid helium II, *Nature (London)* **141**, 75 (1938).
- [3] A. J. Leggett, *Quantum Liquids: Bose Condensation and Cooper Pairing in Condensed-Matter Systems* (Oxford University Press, Oxford, 2006).

- [4] J. F. Annett, *Superconductivity, Superfluids and Condensates*, Oxford Master Series in Physics Vol. 5 (Oxford University Press, Oxford, 2004).
- [5] J. Klaers, J. Schmitt, F. Vewinger, and M. Weitz, Bose-Einstein condensation of photons in an optical microcavity, *Nature (London)* **468**, 545 (2010).

- [6] J. Marelic and R. A. Nyman, Experimental evidence for inhomogeneous pumping and energy-dependent effects in photon Bose-Einstein condensation, *Phys. Rev. A* **91**, 033813 (2015).
- [7] H. Ritsch, P. Domokos, F. Brennecke, and T. Esslinger, Cold atoms in cavity-generated dynamical optical potentials, *Rev. Mod. Phys.* **85**, 553 (2013).
- [8] M. J. Hartmann, F. G. S. L. Brandao, and M. B. Plenio, Quantum many-body phenomena in coupled cavity arrays, *Laser Photon. Rev.* **2**, 527 (2008).
- [9] I. Carusotto, D. Gerace, H. E. Tureci, S. De Liberato, C. Ciuti, and A. Imamoglu, Fermionized photons in an array of driven dissipative nonlinear cavities, *Phys. Rev. Lett.* **103**, 033601 (2009).
- [10] C. Noh and D. G. Angelakis, Quantum simulations and many-body physics with light, *Rep. Prog. Phys.* **80**, 016401 (2017).
- [11] I. Carusotto and C. Ciuti, Quantum fluids of light, *Rev. Mod. Phys.* **85**, 299 (2013).
- [12] H. Deng, H. Haug, and Y. Yamamoto, Exciton-polariton Bose-Einstein condensation, *Rev. Mod. Phys.* **82**, 1489 (2010).
- [13] J. Keeling and N. G. Berloff, Exciton-polariton condensation, *Contemp. Phys.* **52**, 131 (2011).
- [14] M. D. Fraser, S. Höfling, and Y. Yamamoto, Physics and applications of exciton-polariton lasers, *Nat. Mater.* **15**, 1049 (2016).
- [15] D. Sanvitto, Shiny condensates, *Nat. Mater.* **15**, 1047 (2016).
- [16] D. Sanvitto and S. Kéna-Cohen, The road towards polaritonic devices, *Nat. Mater.* **15**, 1061 (2016).
- [17] T. Liew, Electrical spin switching, *Nat. Mater.* **15**, 1053 (2016).
- [18] A. Dreismann, H. Ohadi, Y. del Valle-Inclan Redondo, R. Balili, Y. G. Rubo, S. I. Tsintzos, G. Deligeorgis, Z. Hatzopoulos, P. G. Savvidis, and J. J. Baumberg, A sub-femtojoule electrical spin-switch based on optically trapped polariton condensates, *Nat. Mater.* **15**, 1074 (2016).
- [19] I. A. Shelykh, R. John, D. D. Solnyshkov, and G. Malpuech, Optically and electrically controlled polariton spin transistor, *Phys. Rev. B* **82**, 153303 (2010).
- [20] C. Schneider, A. Rahimi-Iman, N. Y. Kim, J. Fischer, I. G. Savenko, M. Amthor, M. Lerner, A. Wolf, L. Worschech, V. D. Kulakovskii *et al.*, An electrically pumped polariton laser, *Nature (London)* **497**, 348 (2013).
- [21] P. Bhattacharya, B. Xiao, A. Das, S. Bhowmick, and J. Heo, Solid state electrically injected exciton-polariton laser, *Phys. Rev. Lett.* **110**, 206403 (2013).
- [22] A. Imamoglu, R. J. Ram, S. Pau, and Y. Yamamoto, Nonequilibrium condensates and lasers without inversion: Exciton-polariton lasers, *Phys. Rev. A* **53**, 4250 (1996).
- [23] T. C. H. Liew, A. V. Kavokin, and I. A. Shelykh, Optical circuits based on polariton neurons in semiconductor microcavities, *Phys. Rev. Lett.* **101**, 016402 (2008).
- [24] T. Espinosa-Ortega and T. C. H. Liew, Complete architecture of integrated photonic circuits based on and not logic gates of exciton polaritons in semiconductor microcavities, *Phys. Rev. B* **87**, 195305 (2013).
- [25] A. Amo, J. Lefrère, S. Pigeon, C. Adrados, C. Ciuti, I. Carusotto, R. Houdré, E. Giacobino, and A. Bramati, Superfluidity of polaritons in semiconductor microcavities, *Nat. Phys.* **5**, 805 (2009).
- [26] A. Amo, D. Sanvitto, F. P. Laussy, D. Ballarini, E. Del Valle, M. D. Martin, A. Lemaitre, J. Bloch, D. N. Krizhanovskii, M. S. Skolnick *et al.*, Collective fluid dynamics of a polariton condensate in a semiconductor microcavity, *Nature (London)* **457**, 291 (2009).
- [27] A. C. Berceanu, L. Dominici, I. Carusotto, D. Ballarini, E. Cancellieri, G. Gigli, M. H. Szymańska, D. Sanvitto, and F. M. Marchetti, Multicomponent polariton superfluidity in the optical parametric oscillator regime, *Phys. Rev. B* **92**, 035307 (2015).
- [28] D. Sanvitto, F. M. Marchetti, M. H. Szymańska, G. Tosi, M. Baudisch, F. P. Laussy, D. N. Krizhanovskii, M. S. Skolnick, L. Marrucci, A. Lemaitre *et al.*, Persistent currents and quantized vortices in a polariton superfluid, *Nat. Phys.* **6**, 527 (2010).
- [29] K. G. Lagoudakis, M. Wouters, M. Richard, A. Baas, I. Carusotto, R. André, L. S. Dang, and B. Deveaud-Plédran, Quantized vortices in an exciton-polariton condensate, *Nat. Phys.* **4**, 706 (2008).
- [30] M. Wouters and I. Carusotto, Superfluidity and critical velocities in nonequilibrium Bose-Einstein condensates, *Phys. Rev. Lett.* **105**, 020602 (2010).
- [31] J. Keeling, Superfluid density of an open dissipative condensate, *Phys. Rev. Lett.* **107**, 080402 (2011).
- [32] A. Janot, T. Hyart, P. R. Eastham, and B. Rosenow, Superfluid stiffness of a driven dissipative condensate with disorder, *Phys. Rev. Lett.* **111**, 230403 (2013).
- [33] V. N. Gladilin and M. Wouters, Normal and superfluid fractions of inhomogeneous nonequilibrium quantum fluids, *Phys. Rev. B* **93**, 134511 (2016).
- [34] G. Wachtel, L. M. Sieberer, S. Diehl, and E. Altman, Electrodynamical duality and vortex unbinding in driven-dissipative condensates, *Phys. Rev. B* **94**, 104520 (2016).
- [35] J. Keeling, L. M. Sieberer, E. Altman, L. Chen, S. Diehl, and J. Toner, Superfluidity and phase correlations of driven dissipative condensates, in *Universal Themes of Bose-Einstein Condensation*, edited by N. P. Proukakis, D. W. Snoke, and P. B. Littlewood (Cambridge University Press, Cambridge, 2017), p. 205.
- [36] J. Keeling and N. G. Berloff, Condensed-matter physics: Going with the flow, *Nature (London)* **457**, 273 (2009).
- [37] E. Cancellieri, F. M. Marchetti, M. H. Szymańska, and C. Tejedor, Superflow of resonantly driven polaritons against a defect, *Phys. Rev. B* **82**, 224512 (2010).
- [38] A. J. Leggett, Superfluidity, *Rev. Mod. Phys.* **71**, S318 (1999).
- [39] L. Pitaevskii and S. Stringari, *Bose-Einstein Condensation and Superfluidity*, Vol. 164 (Oxford University Press, Oxford, 2016).
- [40] G. Baym, The microscopic description of superfluidity, in *Mathematical Methods in Solid State and Superfluid Theory*, edited by R. C. Clark and G. H. Derrick, Scottish Universities' Summer School (Springer, Edinburgh, 1968), pp. 121–156.
- [41] P. Nozières and D. Pines, *The Theory of Quantum Liquids: Superfluid Bose Liquids* (CRC Press, Boca Raton, 2018).
- [42] A. Griffin, *Excitations in a Bose-Condensed Liquid*, Cambridge Studies in Low Temperature Physics 4 (Cambridge University Press, Cambridge, UK, 1993).
- [43] A. Leggett, On the superfluid fraction of an arbitrary many-body system at  $t = 0$ , *J. Stat. Phys.* **93**, 927 (1998).
- [44] V. G. Rousseau, Superfluid density in continuous and discrete spaces: Avoiding misconceptions, *Phys. Rev. B* **90**, 134503 (2014).
- [45] J. Kasprzak, M. Richard, S. Kundermann, A. Baas, P. Jeambrun, J. Keeling, F. M. Marchetti, M. H. Szymańska, R. André, J. L.

- Stahli *et al.*, Bose-Einstein condensation of exciton polaritons, *Nature (London)* **443**, 409 (2006).
- [46] M. H. Szymańska, J. Keeling, and P. B. Littlewood, Mean-field theory and fluctuation spectrum of a pumped decaying Bose-Fermi system across the quantum condensation transition, *Phys. Rev. B* **75**, 195331 (2007).
- [47] M. Wouters and I. Carusotto, Excitations in a nonequilibrium Bose-Einstein condensate of exciton polaritons, *Phys. Rev. Lett.* **99**, 140402 (2007).
- [48] A. Baas, J.-P. Karr, M. Romanelli, A. Bramati, and E. Giacobino, Quantum degeneracy of microcavity polaritons, *Phys. Rev. Lett.* **96**, 176401 (2006).
- [49] I. Carusotto and C. Ciuti, Probing microcavity polariton superfluidity through resonant Rayleigh scattering, *Phys. Rev. Lett.* **93**, 166401 (2004).
- [50] C. C. I. Carusotto, Quantum fluid effects and parametric instabilities in microcavities, *Phys. Stat. Solidi (b)* **242**, 2224 (2005).
- [51] R. Juggins, J. Keeling, and M. Szymańska, Coherently driven microcavity-polaritons and the question of superfluidity, *Nat. Commun.* **9**, 4062 (2018).
- [52] K. Dunnett and M. H. Szymańska, Keldysh field theory for nonequilibrium condensation in a parametrically pumped polariton system, *Phys. Rev. B* **93**, 195306 (2016).
- [53] A. A. Abrikosov, L. P. Gorkov, and I. E. Dzyaloshinski, *Methods of Quantum Field Theory in Statistical Physics* (Courier Corporation, New York, 2012).
- [54] L. Sieberer, Universality in driven-dissipative quantum many-body systems, Ph.D. thesis, University of Innsbruck (2015).
- [55] V. Hakim, S. Pigeon, and A. Aftalion, Metamorphoses of the flow past an obstacle of a resonantly driven bistable polariton fluid, *Phys. Rev. B* **107**, 045306 (2023).
- [56] P. Stepanov, I. Amelio, J.-G. Rousset, J. Bloch, A. Lemaître, A. Amo, A. Minguzzi, I. Carusotto, and M. Richard, Dispersion relation of the collective excitations in a resonantly driven polariton fluid, *Nat. Commun.* **10**, 3869 (2019).
- [57] F. Claude, M. J. Jacquet, R. Usciati, I. Carusotto, E. Giacobino, A. Bramati, and Q. Glorieux, High-resolution coherent probe spectroscopy of a polariton quantum fluid, *Phys. Rev. Lett.* **129**, 103601 (2022).
- [58] F. Claude, M. J. Jacquet, I. Carusotto, Q. Glorieux, E. Giacobino, and A. Bramati, Spectrum of collective excitations of a quantum fluid of polaritons, *Phys. Rev. B* **107**, 174507 (2023).
- [59] E. Talbot and A. Griffin, High- and low-frequency behaviour of response functions in a Bose liquid: One-loop approximation, *Ann. Phys.* **151**, 71 (1983).
- [60] K. Okada, *Catastrophe Theory and Phase Transitions*, Solid State Phenomena Vol. 34 (Trans. Tech. Publications, Stafa-Zurich, Switzerland, 1993).
- [61] R. Gilmore, Catastrophe theory, in *Encyclopedia of Applied Physics: Volume 3*, edited by G. L. Trigg, E. S. Vera, and W. Greulich (VCH Publishers, New York, 1992), pp. 85–119.
- [62] L. S. Schulman, *Techniques and Applications of Path Integration* (Courier Corporation, New York, 2012).
- [63] L. M. Sieberer, M. Buchhold, and S. Diehl, Keldysh field theory for driven open quantum systems, *Rep. Prog. Phys.* **79**, 096001 (2016).
- [64] J. Lebreuilly and I. Carusotto, Quantum simulation of zero-temperature quantum phases and incompressible states of light via non-Markovian reservoir engineering techniques, *C. R. Phys.* **19**, 433 (2018).
- [65] I. Amelio and I. Carusotto, Perspectives in superfluidity in resonantly driven polariton fluids, *Phys. Rev. B* **101**, 064505 (2020).
- [66] R. P. Feynman and F. Vernon, Jr., The theory of a general quantum system interacting with a linear dissipative system, *Ann. Phys.* **281**, 547 (2000).
- [67] D. Nigro, On the uniqueness of the steady-state solution of the Lindblad–Gorini–Kossakowski–Sudarshan equation, *J. Stat. Mech.* (2019) 043202.
- [68] A. Kamenev, *Field Theory of Non-Equilibrium Systems* (Cambridge University Press, Cambridge, 2011).
- [69] V. Arnold, *Ordinary Differential Equations* (MIT Press, Cambridge, MA, 1973).